Functional Divergence of Mammalian TFAP2a and TFAP2b Transcription Factors for Bidirectional Sleep Control

Yang Hu,* Alejandra Korovaichuk,* Mariana Astiz,† Henning Schroeder,‡ Rezaul Islam,‡ Jon Barrenetxea,* Andre Fischer,‡,§, Henrik Oster,† and Henrik Bringmann*,††,‡‡,1**

*Max Planck Research Group "Sleep and Waking", Max Planck Institute for Biophysical Chemistry, Göttingen 37077, Germany, †Institute of Neurobiology, University of Lübeck, 23562, Germany, ‡German Center for Neurodegenerative Diseases, Göttingen 37075, Germany, §Department for Psychiatry and Psychotherapy, University Medical Center, Göttingen 37075, Germany, **Cluster of Excellence "Multiscale Bioimaging: from Molecular Machines to Networks of Excitable Cells" (MBExC), University of Göttingen, 37073, Germany, ††Department of Animal Physiology/Neurophysiology, Philipps University Marburg, Marburg 35043, Germany, and ‡‡BIOTEC of the Technical University Dresden, Dresden 01307, Germany

ORCID IDs: 0000-0002-2515-4458 (Y.H.); 0000-0001-9912-1686 (M.A.); 0000-0002-1414-7068 (H.O.); 0000-0002-7689-8617 (H.B.)

ABSTRACT Sleep is a conserved behavioral state. Invertebrates typically show quiet sleep, whereas in mammals, sleep consists of periods of nonrapid-eye-movement sleep (NREMS) and REM sleep (REMS). We previously found that the transcription factor AP-2 promotes sleep in *Caenorhabditis elegans* and *Drosophila*. In mammals, several paralogous AP-2 transcription factors exist. Sleep-controlling genes are often conserved. However, little is known about how sleep genes evolved from controlling simpler types of sleep to govern complex mammalian sleep. Here, we studied the roles of *Tfap2a* and *Tfap2b* in sleep control in mice. Consistent with our results from *C. elegans* and *Drosophila*, the AP-2 transcription factors *Tfap2a* and *Tfap2b* also control sleep in mice. Surprisingly, however, the two AP-2 paralogs play contrary roles in sleep control. *Tfap2a* reduction of function causes stronger delta and theta power in both baseline and homeostasis analysis, thus indicating increased sleep quality, but did not affect sleep quantity. By contrast, *Tfap2b* reduction of function decreased NREM sleep time specifically during the dark phase, reduced NREMS and REMS power, and caused a weaker response to sleep deprivation. Consistent with the observed signatures of decreased sleep quality, stress resistance and memory were impaired in *Tfap2b* mutant animals. Also, the circadian period was slightly shortened. Taken together, AP-2 transcription factors control sleep behavior also in mice, but the role of the *AP-2* genes functionally diversified to allow for a bi-directional control of sleep quality. Divergence of AP-2 transcription factors might perhaps have supported the evolution of more complex types of sleep.

KEYWORDS TFAP2; sleep; behavior; EEG; *Mus musculus*

SLEEP is a fundamental state that is defined by behavioral criteria that include the absence of voluntary movement, an increased arousal threshold, relaxed body posture, reversibility, and homeostatic regulation (Campbell and Tobler 1984). By these criteria, sleep has been identified not only in mammals, but also in other vertebrates as well as in invertebrates (Campbell and Tobler 1984; Tobler 1995; Joiner 2016; Bringmann 2018; Keene and Duboue 2018). Sleep in invertebrates is characterized mostly as quiet sleep, with a reduction of neuronal and behavioral activity (Raizen and Zimmerman 2011; Miyazaki *et al.* 2017). In the more complex brains of mammals, two major stages of sleep have been defined. Rapid eye movement sleep (REMS) is characterized by a relatively active brain and muscle paralysis and is also called active sleep. Non-REM sleep (NREMS) is a type of quiet sleep characterized by a strong reduction of brain and muscle activity (Campbell and Tobler 1984). This suggests that sleep appeared first in evolution as a type of quiet sleep

doi: https://doi.org/10.1534/genetics.120.303533
Manuscript received April 29, 2020; accepted for publication July 20, 2020; published Early Online August 7, 2020.
Available freely online through the author-supported open access option.
Supplemental material available at figshare: https://doi.org/10.6084/m9.figshare.12738545.v1.
[1]Corresponding author: Max Planck Research Group Sleep and Waking, Max Planck Institute for Biophysical Chemistry, 37077 Göttingen, Germany. E-mail: Henrik.Bringmann@mpibpc.mpg.de

and then diversified into two types of sleep, which are manifested as NREMS and REMS in mammals (Miyazaki *et al.* 2017).

The molecular biology of sleep has been studied in all major genetic model animals such as mice, zebrafish, fruit flies, and nematodes (Joiner 2016; Miyazaki *et al.* 2017). Genetic analysis indicates that many genes play evolutionarily conserved roles in sleep control (Roberts and Hudson 2009). Thus, genes can be studied across model organisms to solve underlying molecular mechanisms of sleep regulation. For example, a gain-of-function mutation of salt-inducible kinase 3 (SIK-3) called *sleepy* increased NREM sleep in mice (Funato *et al.* 2016). Whereas a loss-of-function mutation of *SIK-3* is lethal in mice, deletion of the *Caenorhabditis elegans SIK-3* homolog *KIN-29* is not lethal, but reduces sleep (Funato *et al.* 2016). It was shown that SIK-3 impacts sleep in *C. elegans* by controlling energy metabolism (Grubbs *et al.* 2019). We previously showed that knockout of the AP-2 transcription factor APTF-1 results in sleep loss in *C. elegans* (Turek *et al.* 2013). The AP-2 family of transcription factors is evolutionarily conserved in both invertebrates and vertebrates (Bringmann 2018). The basic and helix-span-helix (HSH) domains are necessary for DNA binding and dimerization functions, and are highly conserved among all TFAP2 orthologs and paralogues. The N-terminal portion of the protein contains the transactivation domain, which has an amino acid sequence that is poorly conserved among the AP-2 proteins (Williams and Tjian 1991).

AP-2 transcription factors are best known to control ontogenetic processes such as the development of face, limbs, and organs (Moser *et al.* 1997b; Werling and Schorle 2002; Zhao *et al.* 2003; Lin *et al.* 2018). We showed that, in *C. elegans*, APTF-1 is required for the functioning of the sleep-inducing RIS (Ring Interneuron S) neuron. Without APTF-1, crucial sleep-inducing neuropeptides are not expressed in RIS, and, thus, sleep is virtually abolished (Turek *et al.* 2013). Consistent with a conserved role in sleep control, neuronal knockdown of the sole AP-2 homolog in adult *Drosophila* almost completely abolishes night sleep but without affecting day sleep (Kucherenko *et al.* 2016).

In mammals, the AP-2 family consists of five paralogs, AP-2α–AP-2ε, encoded by genes *Tfap2a–Tfap2e*, respectively (Eckert *et al.* 2005). Here, we focus on *Tfap2a* and *b*, which are expressed prominently in neural crest cells starting around embryonic day 8 (E8) during early development of the central nervous system and are still detectable in adult brains (Chazaud *et al.* 1996; Moser *et al.* 1997b; Zhao *et al.* 2003). In humans, mutations affecting the basic domain in AP-2 can lead to the loss of function of these transcription factors. Heterozygous mutation of *Tfap2a* causes branchio-oculo-facial syndrome (BOFS; OMIM#113620) by a mechanism that mostly involves the loss of function of transcription factor activity (Li *et al.* 2013). BOFS is associated with multiple craniofacial abnormalities as well as eye, hearing, and skin defects. To our knowledge, no sleep abnormalities have been reported for BOFS individuals. Loss of *Tfap2a* causes severe developmental problems of the heart, brain, and skeletal systems leading to lethality (Schorle *et al.* 1996; Zhang *et al.* 1996; Brewer *et al.* 2004). *Tfap2a*$^{+/-}$ mice are viable and fertile. Heterozygous deletion is associated with mild developmental defects in craniofacial and brain development, providing a mouse model to study BOFS (Schorle *et al.* 1996; Zhang *et al.* 1996; Kohlbecker *et al.* 2002; Green *et al.* 2015). To our knowledge, *Tfap2a*$^{+/-}$ mice have not yet been tested for sleep abnormalities.

Heterozygous mutation of *Tfap2b* causes Char syndrome (CHAR, OMIM#169100) by either dominant negative or haploinsufficiency mechanisms (Satoda *et al.* 2000; Zhao *et al.* 2001; Mani *et al.* 2005). CHAR is characterized by developmental defects that include facial dysmorphism, abnormalities of the fifth finger, and failure of *ductus arteriosus* closure (patent *ductus arteriosus*, PDA) (Satoda *et al.* 1999). In two families with heterozygous loss of *Tfap2b* function, CHAR individuals showed self-reported sleep abnormalities. In the first family, sleepwalking was reported, whereas in the second family individuals reported shortened nocturnal sleep. However, the nature of these sleep changes remains unclear as these phenotypes were not confirmed using polysomnography (Mani *et al.* 2005). Homozygous deletion of *Tfap2b* in mice causes early lethality. By contrast, heterozygous deletion in mice causes PDA and fifth finger digit abnormalities but no obvious facial anomalies, providing a model of CHAR (Moser *et al.* 1997a; Satoda *et al.* 1999). However, sleep has not yet been studied in *Tfap2b*$^{+/-}$ mice.

AP-2 transcription factors have diverged in mammals to play nonredundant roles in development. In invertebrates, AP-2 plays a key role in sleep induction. Hence, AP-2 transcription factors provide a unique chance to study how sleep genes evolved from controlling simpler types of sleep in invertebrates to more complex types of sleep in mammals. Multiple hypotheses are conceivable for how AP-2 transcription factors may have evolved to control sleep. Three hypotheses may seem most plausible. (1) A sleep-promoting role might be present in one of the AP-2 paralogs, but such a role is not found in other AP-2 paralogs. (2) Multiple AP-2 paralogs might play a redundant role in promoting sleep. (3) Different AP-2 paralogs might serve specialized subfunctions in promoting sleep.

In this study, we studied sleep in *Tfap2a*$^{+/-}$ and *Tfap2b*$^{+/-}$ mice. Surprisingly, we found that *Tfap2a* and *Tfap2b* play opposing roles in sleep control. *Tfap2a*$^{+/-}$ causes an increase in sleep quality, and is also associated with hyperactivity during a stress test. By contrast, *Tfap2b*$^{+/-}$ reduces sleep time and quality and is associated with altered circadian rhythms, mildly depressive-like symptoms, and a learning defect. Thus, AP-2 transcription factors appear to have diverged to allow bidirectional control of sleep.

Materials and Methods

Animals

Neofloxed-*Tfap2a* conditional knockout mice were obtained from Trever Williams (Brewer *et al.* 2004) and bred with

CMV-Cre mice to delete exons 5–6 of *Tfap2a*. Mice that are homozygous for this allele were perinatal lethal in our colony probably due to neural tube closure defects and cleft secondary palate (Zhang *et al.* 1996). Thus, heterozygous mice (*Tfap2a*$^{+/-}$) were used in this study and their wild-type littermates (*Tfap2a*$^{+/+}$) were used as controls.

Tfap2b knockout mice were provided by Markus Moser [Max Planck Institute (MPI) for Biochemistry] with PGK-neo cassette inserted into exon four of the *Tfap2b* gene. *Tfap2b*$^{-/-}$ mice die shortly after birth due to polycystic kidney disease (Moser *et al.* 1997a). Thus, heterozygous mice (*Tfap2b*$^{+/-}$) were used in this study and their wild-type littermates (*Tfap2b*$^{+/+}$) were used as controls.

Adult (2–6 M) males were used in this study, except for the running-wheel test (see section *Wheel-running activity and circadian analysis*). Mice were kept at the animal facility of the MPI of Biophysical Chemistry in accordance to Lower-Saxony animal welfare laws. All animal experiments were carried out in compliance with the German Law on Animal Welfare and were approved by the Office for Consumer Protection and Food Safety of the State of Lower Saxony. All animal experiments were approved by the Animal Experiments Ethical Committee of the Max Planck Institute for Biophysical Chemistry (Göttingen, Germany) and Laves, and were carried out in accordance with European Union (EU) Directive 2010/63/EU on the protection of animals used for scientific reasons. Mice were entrained in a 12:12 hr light-dark cycle from 6:00 to 18:00. For the entire behavioral testing, adult male mice were singly housed with *ad libitum* access to water and food pellets, in controlled constant temperature and humidity. The animals were individually housed at least 1 week prior to the experiment.

Genotyping

Ear biopsies of mice were collected and genomic DNA was extracted through incubation in PBND lysis buffer (PCR buffer with nonionic detergents: 50 mM KCl, 10 mM Tris HCl pH 8.3, 2.5 M $MgCl_2$, 0.1 mg/ml Gelatin, 1 mg/ml proteinase K, 0.45% NP-40, 0.45% Tween) for at least 6 hr at 55°, followed by 45 min at 85° to deactivate the Proteinase K. Genotyping primers and conditions are listed in Supplemental material, Table S1.

Surgeries

Mice were anesthetized using isoflurane (1–2% in 100% O_2) during the surgery. Miniature screw electrodes (2.16 mm diameter, Bilaney Consultants GmbH) with wire (5 mm) attached were implanted. Two electrodes were placed over the right and left frontal cortex [anteroposterior (AP) +1.5 mm from bregma; mediolateral (ML) 1.7 mm). One electrode was placed over the right parietal (AP +1.5 mm from lambda, ML, 1.7 mm) cortex. Two electrodes were placed bilaterally over the cerebellum (AP -1.5 mm from lambda, ML, 1.7 mm) as reference (left) and ground signal (right). One subcutaneous electrode (12 mm, Bilaney Consultants GmbH) was placed in the nuchal muscle for the electromyogram (EMG) recording. All attached wires were assembled in a plastic pedestal (MS363, PlasticsOne, Bilaney Consultants GmbH), which was fixed to the skull with dental cement. The mice were housed individually and left to recover for at least 8 days before they were attached to the recording cable. Mice were given a 2-day acclimation period to adjust to the cable before recording.

Electroencephalogram recording setups and schedule

The recording room was kept under 12 hr light/12 hr dark cycles and room temperature. Light was delivered from ZT0 (6 AM) to ZT12 every day. All electrodes were gathered into a light weight and flexible cable and connected to the recording system (Multi Channel Systems MCS GmbH). Electroencephalogram (EEG) and Electromyography (EMG) signals were collected continuously at a sampling rate of 2000 Hz. To examine the sleep–wake behavior under the baseline conditions, the EEG/EMG recordings were performed for two consecutive days, beginning at ZT0. By the end of the baseline recording, all mice were sleep-deprived (Bernard *et al.* 2015) by gentle handling and novel object interaction protocols for six consecutive hours started from ZT0 to ZT6 (Colavito *et al.* 2013). Any direct contact of the experimenter with the animals was avoided. At the end of the sleep deprivation (SD) period, the animals were left to move and sleep freely with free access to food and water, and recording was continued for the next 48 hr.

EEG data analysis

A MatLab-based, custom-written auto-score system was first trained with EEG/EMG data by a human scorer. The EEG/EMG data were then analyzed by the auto-score system (Gao *et al.* 2016), followed by visual inspection by the same human scorer. In brief, a training set was selected for every 24 hr of data based on a random REMS epoch and preceding 90 epochs (15 min) as well as the following 90 epochs. This process was repeated until a total of 720 epochs (2 hr) of training was selected. The remaining 7920 epochs (22 hr) were subjected to short-time Fourier transformation and auto-scored with a multiple classifier system at a 5% rejection threshold using MatLab. Training and rejected epochs were scored using Sirenia Sleep Pro (Pinnacle Technologies, Lawrence, KS). Manual scoring of three vigilance states were performed for each 10-s epoch as either wake, NREMS and REMS. Wake was scored based on the presence of low amplitude, fast EEG, and high amplitude, variable EMG. NREMS was characterized by high-amplitude delta (0.5–4 Hz) EEG but low frequency EMG activity. REMS was characterized by low-amplitude rhythmic theta waves (6–10 Hz) with EMG atonia. The scorer was blind to the genotype within all the scoring process. The power for each 0.1-Hz bin (between 0.5 and 25 Hz) within the 10-s segment was calculated. For 48 hr of baseline recording, average values were calculated and plotted on a 24 hr-scale. Time spent per hour or total hours in wake/NREMS/REMS stages was calculated over ZT or during the 24 hr light/dark phase for each genotype. To

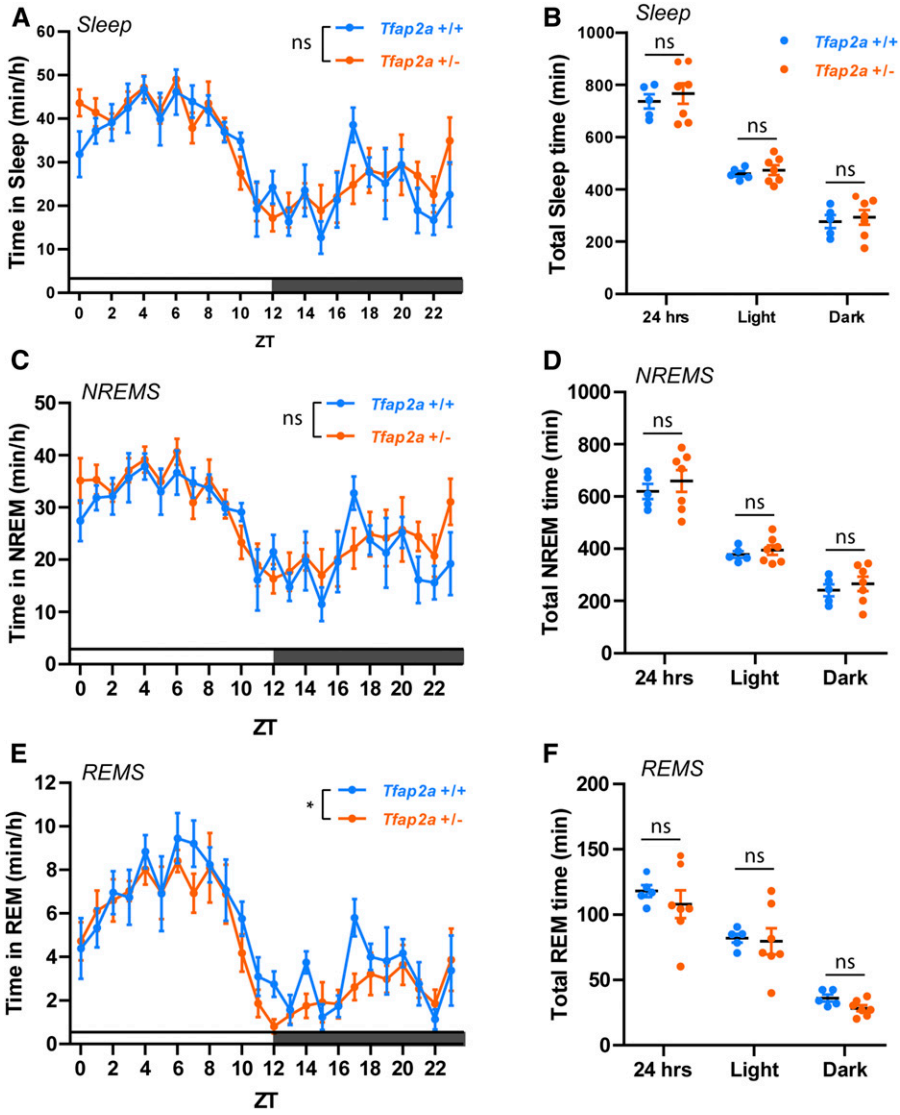

Figure 1 Sleep amount is not significantly altered in *Tfap2a*$^{+/-}$ mice. (A) Total sleep quantification over *Zeitgeber* times (ZT), two-way ANOVA followed by Sidak's multiple comparisons test, the main effect of genotype, F (1,240) = 0.941, P = 0.333. (B) Total sleep time quantification, P = 0.576; light, P = 0.574; dark, P = 0.687. (C) NREMS quantification over ZT, two-way ANOVA followed by Sidak's multiple comparisons test, the main effect of genotype, F (1,10) = 0.526, P = 0.485. (D) NREMS time quantification, P = 0.446; light, P = 0.521; dark, P = 0.543. (E) REMS quantification over ZT, two-way ANOVA followed by Sidak's multiple comparisons test, the main effect of genotype, F (1,239) = 0.492, *P = 0.0353. (F) REMS time quantification, P = 0.466; light, P = 0.852; dark, P = 0.053. n = 5 for *Tfap2a*$^{+/+}$, n = 7 for *Tfap2a*$^{+/-}$. Two-tailed unpaired *t*-tests were used for (B, D, and F). Averaged data are shown as the mean ± SEM.

evaluate the effect of SD, changes in time or bout length of NREMS/REMS during recovery sleep were calculated. In power spectral analysis, the EEG time series were decomposed into a voltage by frequency spectral graph, with power calculated as the square of the EEG magnitude, and magnitude being the integral average of the amplitude of the EEG signal (Kent *et al.* 2018). During baseline recording, derived power data were further grouped and analyzed based on frequency and vigilance states. Here, we presented the raw power data based on the vigilance state in combination with either the distribution of power in 0.1-Hz windows or frequency classes. After SD, the NREMS/REMS/wake powers during recovery sleep were expressed as percentage to the mean of the same ZT from basal recording. Mean values of power spectrum data were calculated for each genotype and the values were submitted to Wilcoxon signed rank tests to make comparison between the genotypes. All power data were expressed as averaged values from measurement of frontal and temporal lobes. For delta and theta power analysis following SD, Z06-12, Z12-18, Z18-24 time zones following the end of SD were used.

Behavioral testing

All behavioral tests were conducted between 08:30 AM and 06:00 PM during the light phase. The order of testing was as follows: elevated plus maze (EPM), rotarod, Morris water maze (MWM), sucrose preference test (SPT), forced swim test (FST), tail suspension test (TST), and fear conditioning (FC).

Elevated plus maze

The EPM consisted of four arms, each 30 cm long and 9.7 cm wide, elevated 50 cm off the ground. Two arms were enclosed by walls 25 cm high and the other two arms were exposed. Mice were placed on the central platform. The behavior of each subject was tracked by an overhead camera and a computer equipped with VideoMot (TSE Systems GmbH, Germany), and recorded for 5 min. VideoMot was

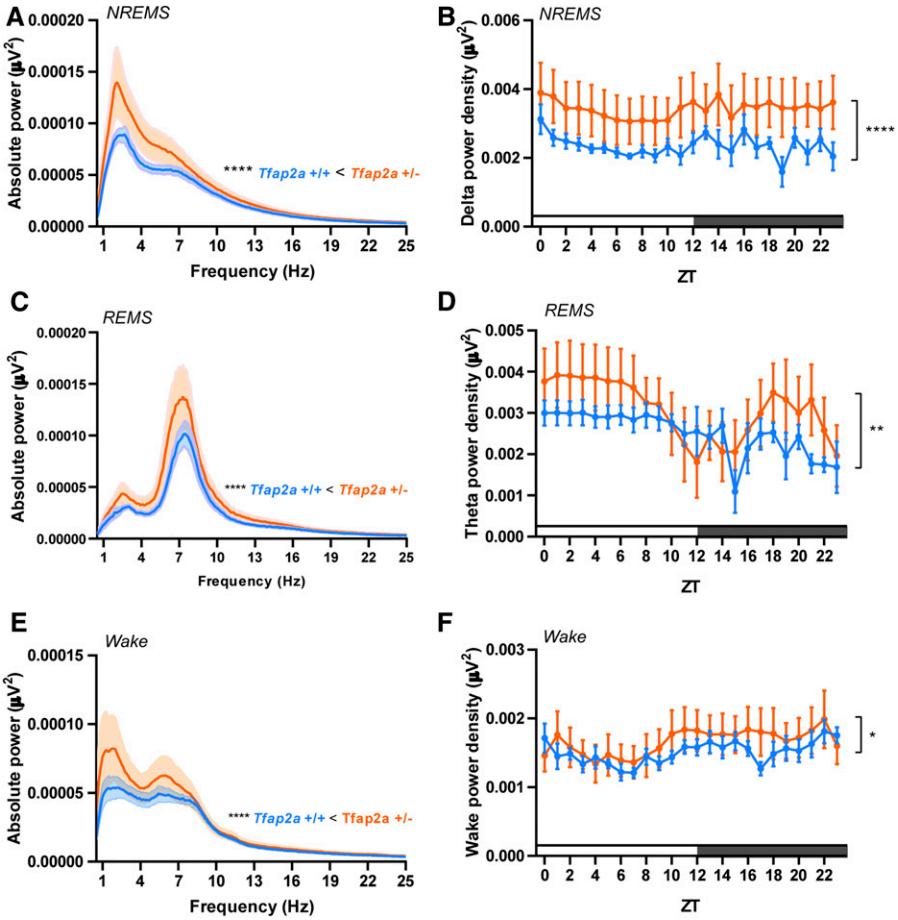

Figure 2 EEG delta and theta power are increased in *Tfap2a*$^{+/-}$ mice. (A) EEG power spectra in NREMS. (B) NREMS delta power (1–4 Hz), two-way ANOVA followed by Sidak's multiple comparisons test, the main effect of genotype, $F(1,240) = 29.58$, $^{****}P < 0.0001$. (C) EEG power spectra in REMS. (D) REMS theta power (6–10 Hz): two-way ANOVA followed by Sidak's multiple comparisons test, the main effect of genotype, $F(1,240) = 7.558$, $^{**}P = 0.0064$. (E) EEG power spectra during wakefulness. (F) Power analysis during wake (0.5–4 Hz), two-way ANOVA followed by Sidak's multiple comparisons test, the main effect of genotype, $F(1,240) = 4.028$, $^{*}P = 0.0459$. All data are shown as the mean ± SEM $n = 5$ for *Tfap2a*$^{+/+}$, $n = 7$ for *Tfap2a*$^{+/-}$. *P* values for 1–25 Hz were calculated using Wilcoxon two-sided signed-rank test, $^{****}P < 0.0001$. All data are shown as the mean ± SEM.

used to calculate the time spent in the open or closed arm. Time spent in open arm or central platform was used to evaluate exposure aversion.

Rotarod test

Motor functions and coordination were examined on the rotarod machine with automatic falling sensors (RotaRod Advanced, TSE Systems GmbH, Germany). For the habituation, mice were trained with the rotating speed of 10 rpm twice a day for two consecutive days. In each trial, mice were placed back to the rod immediately after falling off. After training, mice were tested under continuous acceleration from 5 rpm to 40 rpm with two sessions per day for two consecutive days. The latency to fall was recorded with a computer equipped with RotaRod software. Each measurement lasted 180 s with at least 6-hr intervals.

MWM test

A circular pool of 1.0 m in diameter was used for the MWM. The water (21°), made opaque by addition of nontoxic tempera paint, was 20 cm deep, and the wall of the pool extended 15 cm above the surface of the water. A square hidden platform (13 × 13 cm) was located 1 cm below the water surface approximately in the middle of one of the pool quadrants. Distal visual cues surrounding the pool included four colored labels of different shapes fixed around the edge of the water tank, as well as a door and a wall of cabinets. The test consisted of three phases: visible platform task, hidden platform task and probe test for a total of 11 consecutive days. To exclude mice with visual or motivational impairments and habituate them to the testing conditions, we performed visible platform task during the first 2 days. In this phase, mice were trained to swim to a visible platform placed 1 cm above water surface and in the middle of the water tank. Next, mice were tested with a hidden platform task where a fixed platform was hidden 1.0 cm below the water surface. Mice that failed to locate the platform within 90 sec were guided to it, and all mice were allowed to rest on the platform for at least 15 sec before being returned to their cage. On probe test day, the platform was removed, and mice were allowed to swim in the pool for up to 90 sec. The time spent in each quadrant was measured. On each of the 11 days, mice were given four trials per day starting from each of the four cardinal directions (N, S, E, W) in a pseudorandom order that changed every day. In each trial, mice were gently held close to the water surface facing the wall and then placed in the pool. The swim patterns were monitored by the video-tracking system VideoMot (TSE Systems GmbH). The escape latency, swim speed, path length, and

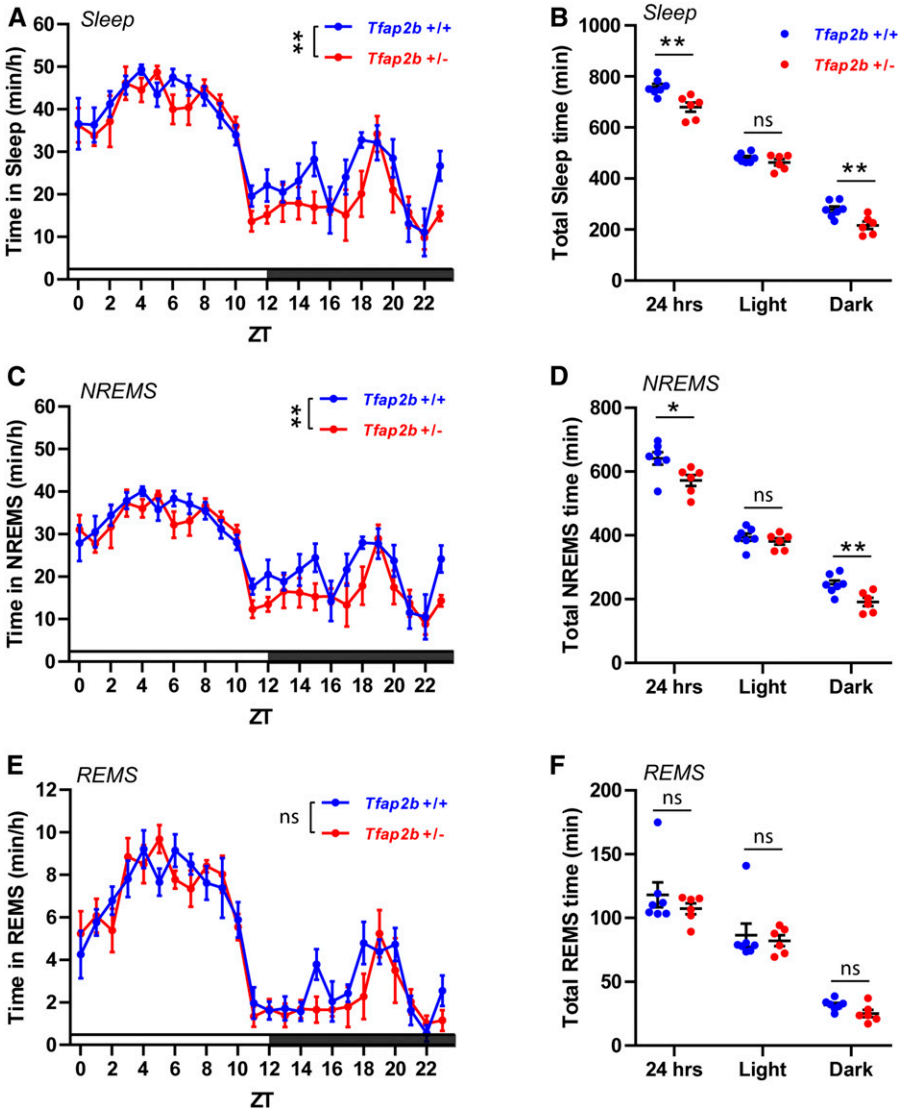

Figure 3 Sleep during the dark phase is reduced in *Tfap2b*$^{+/-}$ mice. (A) Total sleep time quantification over ZT, two-way ANOVA followed by Sidak's multiple comparisons test, the main effect of genotype, F (1,264) = 10.01, $^{**}P$ = 0.002. (B) Total sleep time quantification, $^{**}P$ = 0.004; light, P = 0.222; dark, $^{**}P$ = 0.007. (C) NREMS quantification over ZT, two-way ANOVA followed by Sidak's multiple comparisons test, the main effect of genotype, F (1,264) = 10.26, $^{**}P$ = 0.002. (D) NREMS total time quantification, $^{*}P$ = 0.024; light, P = 0.411; dark, $^{**}P$ = 0.008. (E) REMS quantification over ZT, two-way ANOVA followed by Sidak's multiple comparisons test, the main effect of genotype, F (1,263) = 1.492, P = 0.223. (F) REMS total time quantification, P = 0.668; light, P = 1.000; dark, P = 0.055. n = 7 for *Tfap2b*$^{+/+}$, n = 6 for *Tfap2b*$^{+/-}$. Two-tailed unpaired t-tests were used for (B, D, and F). All data are shown as the mean ± SEM.

trajectory of swimming were recorded for each mouse. Mice that were swimming slower than 60% of the average speed of wild type, *Tfap2a*, and *Tfap2b* mutants during each phase were classified as floaters. Two floaters were removed from the *Tfap2a*$^{+/-}$, eight from *Tfap2b*$^{+/+}$, six from *Tfap2b*$^{+/-}$.

Sucrose preference test

The whole experiment was carried out in the home cage of the mice in the breeding area. Two identical bottles were used for each cage and placed in left and right sides of the cage. Mice were allowed to habituate to the bottles with standard drinking water for 48 hr. In the second 24 hr of the habituation period, weights of the bottles were recorded. Then, mice were given 48 hr of free choice between two bottles of either 2% sucrose or standard drinking water. At the end of the period the bottles were weighed again and the consumption was calculated. No previous food or water deprivation was applied before the test. The percentage of sucrose preference was calculated using the following formula: Sucrose preference = V(sucrose solution)/[V(sucrose solution)+V(water)] × 100%.

Forced swim test

The test apparatus consisted of an inescapable transparent cylinder (25 cm height × 15 cm diameter) containing 20 cm of water (23°). Dividers (35 cm height × 22 cm width) were used between cylinders to prevent mice from seeing each other during the test. Mice were individually placed into the cylinders, and the immobility was recorded over a 6-min test period. Immobility was analyzed by an observer according to the following criteria. Each mouse was judged to be immobile when it ceased struggling and remained floating motionlessly in the water, making only those movements necessary to keep its head above water.

Tail suspension test

The TST (Gibney *et al.* 2013) was performed as described previously (Can *et al.* 2012). Each mouse was suspended

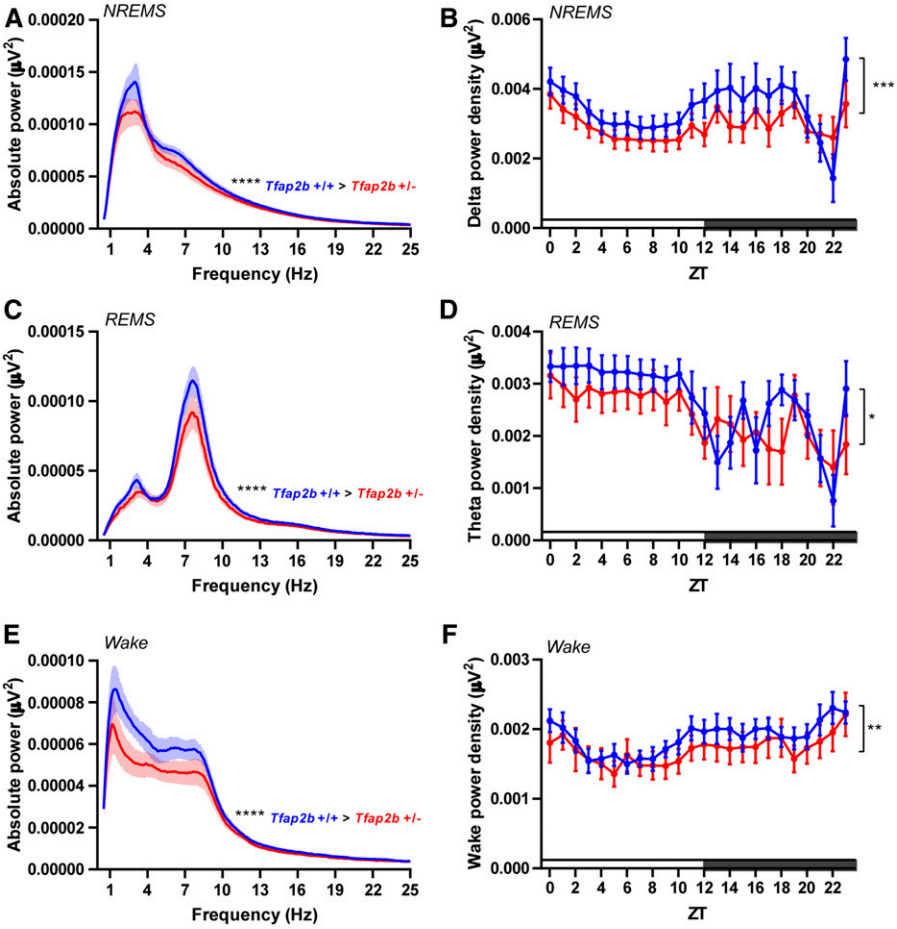

Figure 4 EEG delta and theta power are decreased in *Tfap2b*$^{+/-}$ mice. (A) EEG power spectra in NREMS. (B) NREMS delta power (1–4 Hz), two-way ANOVA followed by Sidak's multiple comparisons test, the main effect of genotype, F (1,264) = 13.68, ***P = 0.0003. (C) EEG power spectra in REMS. (D) REMS theta power (6–10 Hz), two-way ANOVA followed by Sidak's multiple comparisons test, the main effect of genotype, F (1,264) = 5.525, *P = 0.0195. (E) EEG power spectra during wakefulness. (F) Wake power analysis (0.5–4 Hz), two-way ANOVA followed by Sidak's multiple comparisons test, the main effect of genotype, F (1,264) = 9.126, **P = 0.0028. All data are shown as the mean ± SEM, n = 7 for *Tfap2b*$^{+/+}$, n = 6 for *Tfap2b*$^{+/-}$. P values for 1–25 Hz were calculated using Wilcoxon two-sided signed-rank test, ****P < 0.0001. All data are shown as the mean ± SEM.

30 cm above the floor by the tail with a 16 cm long piece of tape. Dividers (35 cm height × 15 cm width) were hanged between tapes to prevent mice from seeing each other during the test. The behavior was recorded for 6 min. Immobility was analyzed by an observer.

Contextual FC test

The contextual FC test was performed as described previously (Fischer *et al.* 2004; Sananbenesi *et al.* 2007). In brief, FC was carried out with a computerized fear conditioning system (TSE Systems GmbH) using a computer, equipped with Freeze Scan software (Clever Systems), connected to a control unit containing a shock and a noise generator. Animals were allowed to explore the training cage for 3 min followed by a mild electric shock (2 sec, 0.5 mA). Context-dependent freezing, defined as the absence of movements other than those required for breathing, was assessed for the following 2 days with a 24-hr interval without the electric shock. Freezing behavior and average movement were recorded for each mouse.

Wheel-running activity and circadian analysis

The setup included six controls and six mutant mice (three males and three females for each genotype of *Tfap2a* and *Tfap2b*) at the age of 2–5 months. Mice were placed in single cages with running wheels connected to a computer running ClockLab (Actimetrics) data collection software. Genotypes and sexes were evenly distributed over two boxes. Animals were not disturbed during the entire experiment. Wheel counts were checked every day to assess well-being of the animal. The experiment consisted of five phases: training phase, entrainment phase, phase advance (jetlag), light pulse at ZT14, and free-running phase. During the training phase, animals were in a 12 hr light: 12 hr dark (LD) cycle for >7 days with a light phase light intensity of 300 lux to habituate to the running-wheel. Next, daily activities were recorded and calculated as an average of 10 days. After the entrainment period in LD, mice were subjected to an abrupt shift in the light schedule by advancing the "lights off" time by 6 hr (jetlag paradigm). The number of days needed to completely re-entrain to the shifted LD cycle was compared between the genotypes. After mice were completely re-entrained to the new LD cycle, a light pulse was delivered at ZT14 for 30 min at 300 lux and mice released into constant darkness (DD), and phase shifts were calculated for activity onsets on the day after the light pulse. Mice were retained in DD for another 2 weeks to assess free-running period lengths by χ^2 periodogram analysis. One female in

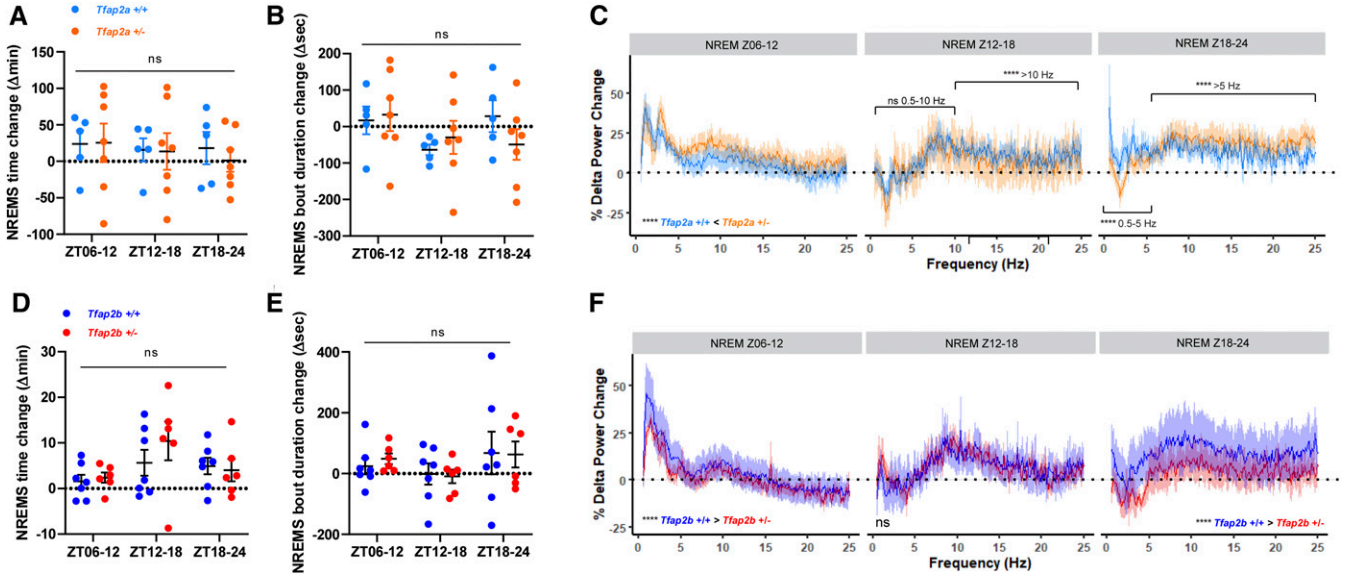

Figure 5 NREMS delta power following sleep deprivation is increased more strongly in *Tfap2a*$^{+/-}$ mice but less strongly in *Tfap2b*$^{+/-}$ mice. (A) NREMS time change in *Tfap2a*$^{+/-}$, two-way ANOVA tests followed by Sidak's pairwise comparison, the main effect of genotype: F(1, 30) = 0.103, $P = 0.750$; the main effect of time, F(2, 30) = 0.791, $P = 0.791$. (B) Average NREMS bout duration change in *Tfap2a*$^{+/-}$, two-way ANOVA tests followed by Sidak's pairwise comparison, the main effect of genotype: F(1, 30) = 0.072, $P = 0.790$; the main effect of time, F(2, 30) = 1.407, $P = 0.261$. (C) NREMS delta power changes (0.5–25 Hz) in *Tfap2a*$^{+/-}$ mice. Z06-12: 0.5–25 Hz, ****$P < 0.0001$. Z12-18: 0.5–10 Hz, $P = 0.334$; 10–25 Hz, ****$P < 0.0001$. Z18–24: 0.5–5 Hz, $P = 0.334$; 5–25 Hz, ****$P < 0.0001$. (D) NREMS time change in *Tfap2b*$^{+/-}$, two-way ANOVA tests followed by Sidak's pairwise comparison, the main effect of genotype: F(1, 33) = 0.595, $P = 0.446$; the main effect of time, F(2, 33) = 3.008, $P = 0.063$. (E) Average NREMS bout duration change in *Tfap2b*$^{+/-}$, two-way ANOVA tests followed by Sidak's pairwise comparison, the main effect of genotype: F(1, 33) = 0.014, $P = 0.906$; the main effect of time, F(2, 33) = 1.476, $P = 0.243$. (F) NREMS delta power changes (0.5–25 Hz) in *Tfap2b*$^{+/-}$ mice. Z06–12: 0.5–25Hz, ****$P < 0.0001$. Z12–18: 0.5–25 Hz, $P = 0.715$. Z18–24: 0.5–25 Hz, ****$P < 0.0001$. $n = 5$ for *Tfap2a*$^{+/+}$, $n = 7$ for *Tfap2a*$^{+/-}$, $n = 7$ for *Tfap2b*$^{+/+}$, $n = 6$ for *Tfap2b*$^{+/-}$. Wilcoxon two-sided signed-rank tests were used for power changes in (C and F). BSL, baseline sleep; R, recovery sleep. All data are shown as the mean ± SEM.

Tfap2a$^{+/+}$ was identified as an outlier using ROUT ($Q = 1\%$) method and was removed from further analyses.

RNA-sequencing

RNA isolation and sequencing were carried out by Bernd Timmermann and Stefan Börno at the sequencing facility of the Max Planck Institute for Molecular Genetics, Berlin, according to their protocol: RNA was isolated from 20 to 80 mg of mouse brain tissue from B6N, *Tfap2a*$^{+/-}$ and *Tfap2b*$^{+/-}$ (stored in RNAlater) following the Qiagen RNeasy protocol. First, the tissue samples were homogenized with the TissueLyser (Qiagen) at 25 Hz for 2 × 2 min in Qiazol lysis buffer; 140 µl chloroform was added, and, after 15 min centrifugation at 12,000 × *g*, the aqueous phase containing the RNA was extracted. Ethanol (1.5 volumes) was added and the samples were washed with Qiagen's RWT buffer on a Qiagen RNeasy spin column. RNA was treated with 10 µl of DNase I on column for 15 min followed by a wash with RWT. After further washes with RPE buffer, the purified RNA was eluted with 50 µl water, yielding between 5 and 22 µg RNA.

After quality control using Agilent's Bioanalyzer, sequencing libraries were prepared from 500 ng of total RNA per sample following Roche's stranded "KAPA RNA HyperPrep" library preparation protocol for single indexed Illumina libraries: First, the polyA-RNA fraction was enriched using oligo-dT-probed paramagnetic beads. Enriched RNA was heat-fragmented and subjected to first-strand synthesis using random priming. The second strand was synthesized incorporating dUTP instead of dTTP to preserve strand information. After A-tailing, Illumina sequencing compatible adapters were ligated. Following bead-based clean-up steps, the libraries were amplified using 11 cycles of PCR. Library quality and size was checked with qBit, Agilent Bioanalyzer, and quantitative PCR (qPCR). Sequencing was carried out on an Illumina HiSeq 4000 system in PE75bp mode, yielding between 27 and 37 million fragments per sample.

Data analysis of RNA-sequencing

Following base calling, adaptor clipping was performed using cutadapt 2.4 (Martin 2011). Data were mapped against the GRCm38.p6 genome using STAR v 2.6.1d (Dobin *et al.* 2013) and differentially expressed genes were analyzed using EdgeR.

Statistics

Statistical analysis was performed using GraphPad Prism 8.3.0 and IBM SPSS (Version 22). All data were subjected to a Shapiro-Wilk normality test for Gaussian distribution and Levene's test for equality of variances. For the dataset that showed a Gaussian distribution ($P > 0.05$ in normality test), we performed parametric tests such as two-tailed

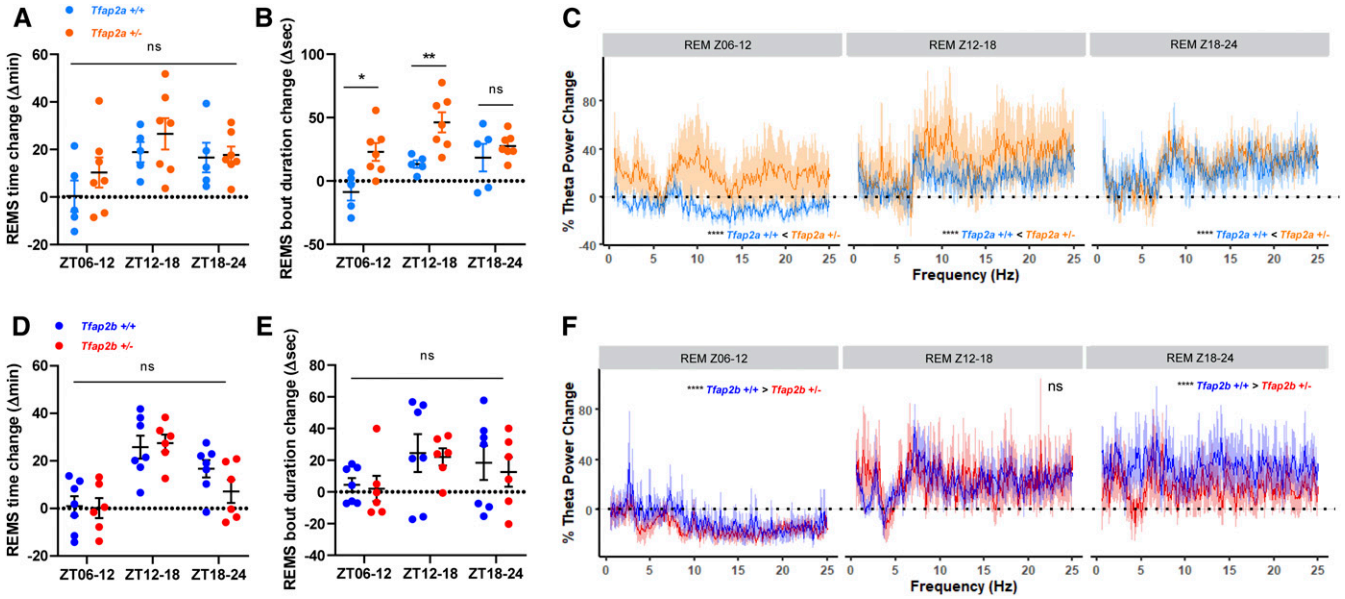

Figure 6 REMS theta power following sleep deprivation is increased more strongly in *Tfap2a*$^{+/-}$ mice but less strongly in *Tfap2b*$^{+/-}$ mice compared with wild-type controls. (A) REMS time change in *Tfap2a*$^{+/-}$, two-way ANOVA tests followed by Sidak's pairwise comparison, the main effect of genotype: $F(1, 30) = 1.698$, $P = 0.202$; the main effect of time, $F(2, 30) = 4.585$, $P = 0.018$. (B) Average REMS bout duration change in *Tfap2a*$^{+/-}$, two-way ANOVA tests followed by Sidak's pairwise comparison, the main effect of genotype: $F(1, 30) = 17.95$, $P = 0.010$; the main effect of time, $F(2, 30) = 5.365$, $P = 0.0002$. ZT06–12: $^{*}P = 0.011$. Z12–18: $^{**}P = 0.0079$. Z18–24: $P = 0.749$. (C) Rebound differences of REMS in theta power (0.5–25 Hz) in *Tfap2a*$^{+/-}$. Z06–12: 0.5–25 Hz, $^{****}P < 0.0001$. Z12–18: 0.5–25 Hz, $^{****}P < 0.0001$. Z18–24: 0.5–25 Hz, $^{****}P < 0.0001$. (D) REMS time change in *Tfap2b*$^{+/-}$, two-way ANOVA tests followed by Sidak's pairwise comparison, the main effect of genotype: $F(1, 33) = 0.673$, $P = 0.418$; the main effect of time, $F(2, 33) = 16.86$, $P < 0.0001$. (E) Average REMS bout duration in *Tfap2b*$^{+/-}$, two-way ANOVA tests followed by Sidak's pairwise comparison, the main effect of genotype: $F(1, 33) = 0.234$, $P = 0.632$; the main effect of time, $F(2, 33) = 2.521$, $P = 0.096$. (F) Rebound differences of REMS in theta power (0.5–25 Hz) in *Tfap2b*$^{+/-}$. Z06–12: 0.5–25 Hz, $^{****}P < 0.0001$. Z12–18: 0.5–25 Hz, $P = 0.119$. Z18–24: 0.5–25 Hz, $^{****}P < 0.0001$. $n = 5$ for *Tfap2a*$^{+/+}$, $n = 7$ for *Tfap2a*$^{+/-}$, $n = 7$ for *Tfap2b*$^{+/+}$, $n = 6$ for *Tfap2b*$^{+/-}$. Wilcoxon two-sided signed-rank tests were used for power changes in (C and F). BSL, baseline sleep; R, recovery sleep. All data are shown as the mean ± SEM.

paired/unpaired *t*-test and ANOVA followed by Sidak's multiple comparisons. For the dataset that failed to show a Gaussian distribution, we performed nonparametric tests, such as a Mann-Whitney test and Wilcoxon signed-rank test. Significance levels in the figures are represented as $^{*}P < 0.05$, $^{**}P < 0.01$, $^{***}P < 0.001$, and $^{****}P < 0.0001$. Error bars in the graphs represent mean ± SEM.

Quantitative PCR

To assess the mRNA reduction of AP-2α and β in *Tfap2a* and *b* mice, total RNA was extracted from the cortex using an RNA extraction kit (Qiagen GmbH). Total RNA was reverse transcribed into cDNA using the high capacity cDNA RT kit (Applied Biosystems) according to the manufacturer's instructions. Subsequently, the mRNA expression levels of AP-2α and β were quantified by qPCR using the Fast SYBR Green Master Mix (Applied Biosystems) using specific primers for each gene (Table S2). cDNA amplification was performed following a PCR program of 40 cycles, with denaturation at 94° for 1 min and annealing at 62° for 30 sec, followed by elongation at 72° for 1 min using an ABI 7500 qPCR cycler. mRNA expression was analyzed using the $2^{-\Delta\Delta Cq}$ method where the control was normalized to 1, and the treated samples were compared with their control. Primers and conditions are listed in Table S2.

Data availability

The authors state that all data necessary for confirming the conclusions presented in the article are represented fully within the article. All data are available at Dryad: https://doi.org/10.5061/dryad.rv15dv45r. Raw RNA-seq data are available at GEO: https://www.ncbi.nlm.nih.gov/geo/query/acc.cgi?acc=GSE155629. EEG-autoscore code is available at GitHub: https://zenodo.org/badge/latestdoi/240526669.

Results

Increased sleep pressure in Tfap2a$^{+/-}$ *mice*

We first analyzed sleep in *Tfap2a* mice. To quantify sleep and wake, we used EEG and EMG recordings (Mang and Franken 2012). As homozygous knockouts of *Tfap2a* are not viable (Zhang *et al.* 1996), we studied *Tfap2a* heterozygous animals. qPCR showed that these mutants had a reduced *Tfap2a* mRNA amount by about half (Supplemental Material, Figure S1). We first analyzed the amount of NREMS and REMS from the electrophysiological recordings. Total sleep time was not significantly affected (Figure 1, A and B). We observed a trend toward increased NREMS (Figure 1, C and D), which did not, however, reach statistical significance. REMS time was decreased slightly (Figure 1, E and F). Sleep

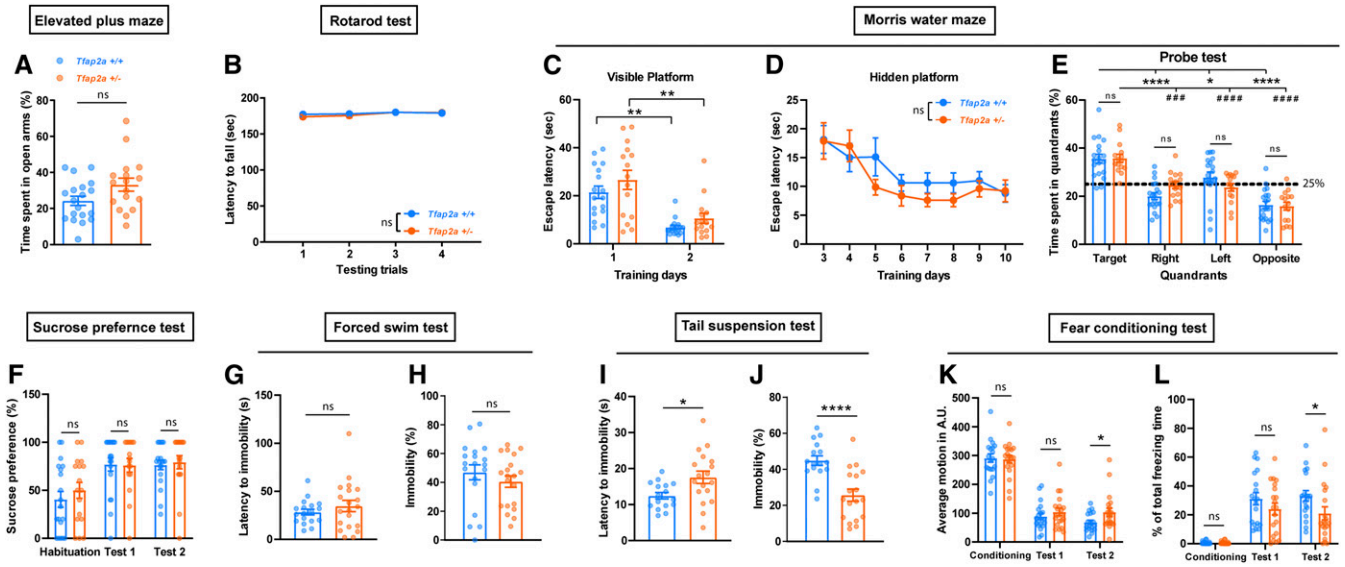

Figure 7 Behavioral phenotyping of *Tfap2a*$^{+/-}$ mice reveals signs of mild hyperactivity. (A) Elevate plus maze, two-tailed unpaired *t*-test, $P = 0.136$. (B) Rotarod test, two-way ANOVA test, the main effect of genotype: $F(1, 148) = 0.927$, $P = 0.337$; the main effect of time, $F(3, 148) = 2.512$, $P = 0.061$. (C) Morris water maze (MWM), time spent searching for visible platform during two consecutive training days: to compare mutants and their controls, unpaired Student *t*-test was used for day 1, $P = 0.274$; Mann-Whitney *U*-test for day 2, $P = 0.096$. Wilcoxon two-sided signed-rank tests for two related samples were used for day 1 and day 2 within each genotype: *Tfap2a*$^{+/+}$, $^{**}P = 0.001$; *Tfap2a*$^{+/-}$, $^{**}P = 0.004$. (D) MWM, time spent searching for hidden platform during eight consecutive training days from day 3 to day 10. Two-way ANOVA tests followed by Sidak's pairwise comparison, the main effect of genotype: $F(1, 256) = 1.049$, $P = 0.307$; the main effect of time, $F(7, 256) = 8.652$, $P < 0.0001$. (E) MWM, time spent in each quadrant during probe test: one-way ANOVA followed by Sidak's pairwise comparison, $F = 21.125$, $P < 0.0001$. *Tfap2a*$^{+/+}$ *vs.* *Tfap2a*$^{+/-}$: target, $P = 1.000$; right, $P = 0.819$; left, $P = 0.918$; opposite, $P = 1.000$. Target *vs.* right/left/opposite quadrant in *Tfap2a*$^{+/+}$: $^{****}P < 0.0001$, $^{*}P = 0.024$, $^{****}P < 0.0001$. Target *vs.* right/left/opposite in *Tfap2a*$^{+/-}$: $^{\#\#\#}P = 0.001$, $^{\#\#\#\#}P < 0.0001$, $^{\#\#\#\#}P < 0.0001$. (F) Sucrose preference test: habituation, $P = 0.379$; test 1, $P = 0.781$; test 2, $P = 0.415$, Mann Whitney test. (G) Forced swim test (FST), latency to immobility, $P = 0.830$, Mann Whitney test. (H) FST, time spent immobile, $P = 0.147$, Mann Whitney test. (I) Tail suspension test (TST), latency to immobility, $^{*}P = 0.039$, Mann Whitney test. (J) TST, time spent immobile, $^{****}P < 0.0001$, Mann Whitney test. (K) Fear conditioning test, average motion, training, $P = 0.296$; test 1, $P = 0.428$; test 2, $^{*}P = 0.028$, Mann Whitney test. (L) Total freezing time, training, $P = 0.771$; test 1, $P = 0.258$; test 2, $^{*}P = 0.018$, Mann Whitney test. Data are shown as the mean ± SEM $n \geq 16$ for *Tfap2a*$^{+/+}$, $n \geq 15$ for *Tfap2a*$^{+/-}$.

bout analysis did not show any significant changes in sleep architecture (Figure S2). We next investigated sleep quality using power spectrum analysis. *Tfap2a*$^{+/-}$ mice exhibited significantly increased delta power in NREMS (Figure 2, A and B) and theta power in REMS (Figure 2, C and D). Additionally, EEG spectral analysis of *Tfap2a*$^{+/-}$ mice during wakefulness showed increased low-frequency power (1–7 Hz) (Figure 2, E and F). Increased delta power in NREMS and increased theta power in REMS suggests that sleep intensity in *Tfap2a*$^{+/-}$ mice was increased.

Sleep loss and reduced sleep quality in Tfap2b$^{+/-}$ *mice*

We next determined sleep amount and quality of *Tfap2b*$^{+/-}$ mice by EEG/EMG recordings. Heterozygous deletion of *Tfap2b* led to a reduction of mRNA by about half (Figure S1). Total sleep time was significantly reduced, an effect that was caused by a specific reduction of sleep during the dark phase (Figure 3, A and B). Analysis of NREMS showed that the reduction of total sleep was due mainly to a reduction in NREMS during the dark phase (Figure 3, C and D). By contrast, no difference could be detected for REMS (Figure 3, E and F). We next analyzed the distribution of sleep bouts in *Tfap2b*$^{+/-}$ mice. Longer sleep bouts were reduced, an effect that was particularly pronounced in the dark phase (Figure S3, A–D). NREMS bouts, particularly long ones, were significantly reduced, again most strongly in the dark phase (Figure S3, E–H). The distribution of REMS bouts remained unchanged (Figure S3, I–L). Power analysis showed that *Tfap2b*$^{+/-}$ mice had significantly decreased delta power in NREMS (Figure 4, A and B), as well as reduced theta power in REMS (Figure 4, C and D). Delta power was already reduced during wakefulness (Figure 4, E and F). In summary, these findings suggest that, in contrast to *Tfap2a*$^{+/-}$ mutants, *Tfap2b*$^{+/-}$ mice have reduced total sleep, which primarily is a consequence of reduced or shortened NREMS bouts in the dark phase. *Tfap2b*$^{+/-}$ mice have less NREMS/REMS power, suggesting a reduction not only of sleep amount, but also of sleep quality.

Opposing effects of Tfap2a$^{+/-}$ *and Tfap2b*$^{+/-}$ *on homeostatic responses to SD*

Baseline sleep characterization showed that reductions in the function of *Tfap2a* and *Tfap2b* have opposing roles in sleep regulation. To test whether these different roles of the two transcription factors extend to sleep homeostasis, we tested the response of *Tfap2a*$^{+/-}$ and *Tfap2b*$^{+/-}$ mice to SD. Using

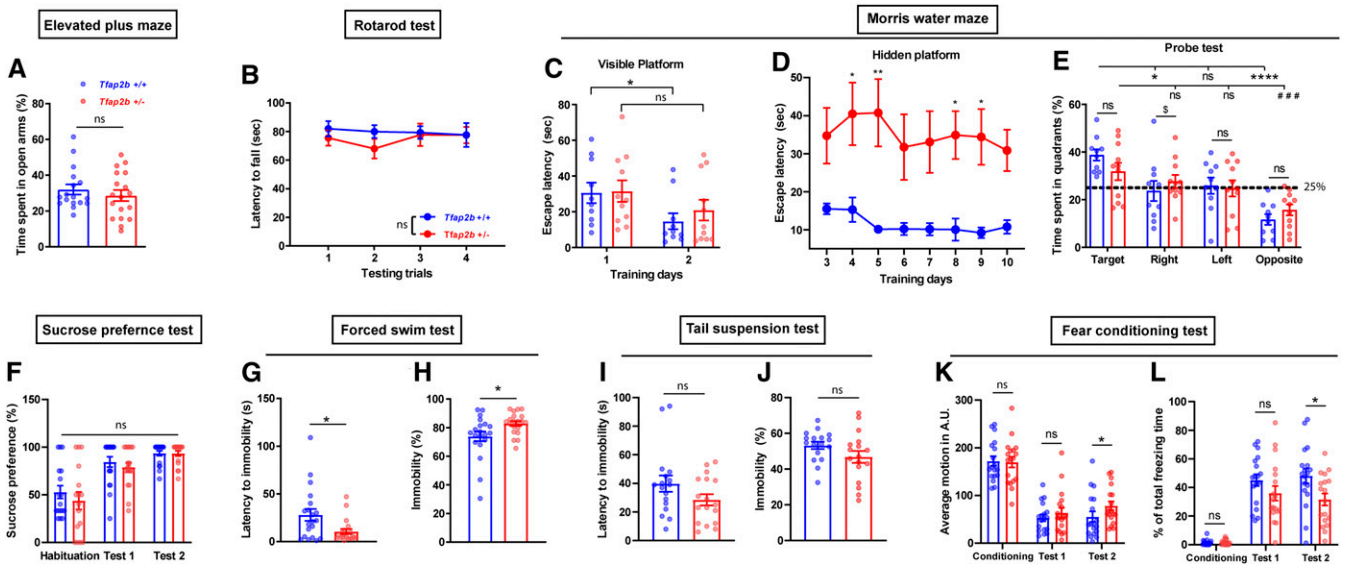

Figure 8 Behavioral phenotyping of *Tfap2b*$^{+/-}$ mice reveals signs of mild depressive-like symptoms. (A) Elevated plus maze, $P = 0.463$, Mann Whitney test. (B) Rotarod test, two-way ANOVA test, the main effect of genotype: F(1, 136) = 1.313, $P = 0.254$; the main effect of time, F(3, 136) = 0.249, $P = 0.862$. (C) Morris water maze (MWM), time spent searching for visible platform during two consecutive training days: to compare mutants and their controls, unpaired Student *t*-test was used for day 1, $P = 0.908$; Mann-Whitney *U*-test for day 2, $P = 0.557$. Wilcoxon two-sided signed-rank tests for two related samples were used for day 1 and day 2 within each genotype: *Tfap2b*$^{+/+}$, $^{*}P = 0.028$; *Tfap2b*$^{+/-}$, $P = 0.091$. (D) MWM, time spent searching for hidden platform during eight consecutive training days, Two-way ANOVA tests, the main effect of genotype: F(1, 148) = 63.40, $P < 0.0001$; the main effect of time, F(7, 148) = 0.377, $P = 0.915$; Sidak's pairwise comparison between genotype,$^{*}P < 0.05$,$^{**}P < 0.01$. (E) MWM, time spent in each quadrant during probe test, one-way ANOVA followed by Sidak's pairwise comparison, F = 7.381, $P < 0.0001$. *Tfap2b*$^{+/+}$ *vs.* *Tfap2b*$^{+/-}$: target, $P = 1.000$; right, $\$P = 0.034$; left, $P = 0.141$; opposite, $P = 1.000$. Target *vs.* right/left/opposite quadrant in *Tfap2b*$^{+/+}$: $^{*}P = 0.034$, $P = 0.141$, $^{****}P < 0.0001$. Target *vs.* right/left/opposite in *Tfap2b*$^{+/-}$: $P = 1.000$, $P = 0.950$, $^{\#\#\#}P = 0.009$. (F) Sucrose preference test, habituation, $P = 0.465$; test 1, $P = 0.372$; test 2, $P = 0.961$, Mann Whitney test. (G) Forced swim test (FST), latency to immobility, $^{*}P = 0.039$, Mann-Whitney test. (H) FST, time spent immobile, $^{*}P = 0.020$, Mann-Whitney test. (I) Tail suspension test, latency to immobility, $P = 0.231$, Mann-Whitney test. (J) Tail suspension test, time spent immobile, $P = 0.087$, Mann-Whitney test. (K) Fear conditioning test, average motion, training, $P = 0.815$; test 1, $P = 0.673$; test 2, $^{*}P = 0.047$, Mann Whitney test. (L) Fear conditioning test, total freezing time, training, $P = 0.696$; test 1, $P = 0.152$; test 2, $^{*}P = 0.027$. Mann Whitney test. All data are shown as the mean ± SEM $n \geq 10$ for *Tfap2b*$^{+/+}$, $n \geq 11$ for *Tfap2b*$^{+/-}$.

gentle handling (Colavito *et al.* 2013), we kept mice awake for 6 hr starting from light onset and measured and quantified the increase in sleep amount and quality by EEG.

Sleep time and delta power increased after SD in all conditions tested (Figures S4 and S5), but the magnitude of delta power responses differed in the different mutants. *Tfap2a*$^{+/-}$ mutant and control animals did not show statistically significant differences in sleep time and bout length (Figure 5, A and B). However, mutant animals exhibited higher rebound delta power compared to control animals within the first 6 hr after SD (Z06–12) (Figure 5C). The delta power rebound diminished during the next (Z12–18) and following 6 hr periods (Z18–24) in both control and mutant animals (Figure 5C). *Tfap2b*$^{+/-}$ animals also showed no difference in NREMS time (Figure 5D) or bout duration (Figure 5E) after SD compared to control animals, but lower rebound delta power during Z06–12 (Figure 5F). During Z12–18, no rebound was observed in both control and mutant animals, but the power change was smaller in mutants during Z18–24 (Figure 5F).

We next quantified REMS time and theta power following SD. A delayed REMS rebound was observed in both *Tfap2a* and *Tfap2b* mutants for REMS time as well as for theta power (Figure S6 and S7). REMS bout duration increased more strongly in *Tfap2a*$^{+/-}$ compared to wild-type littermates ($P < 0.01$) (Figure 6, A and B). *Tfap2a*$^{+/-}$ also showed a higher theta power rebound compared to their littermates (Figure 6C). In contrast, REMS time and REMS bout duration increased less in *Tfap2b*$^{+/-}$ after SD compared to wild-type controls during ZT18-24, although these differences were not significant (Figure 6, D and E). Supporting this trend, the theta power rebound after SD in *Tfap2b*$^{+/-}$ mice was significantly weaker compared to wild-type control animals during Z06-12 and Z18-24 (Figure 6F). Thus, *Tfap2a*$^{+/-}$ mice respond more strongly to SD, whereas *Tfap2b*$^{+/-}$ animals exhibit a weaker response to SD compared to wild-type controls.

Divergent behavioral changes in Tfap2a$^{+/-}$ *and Tfap2b*$^{+/-}$ *mice*

Sleep loss is correlated with emotional instability, anxiety (Verbitsky 2017), depression (Matsuda *et al.* 2017), and cognitive defects (Bezdicek *et al.* 2018). We hence tested how reduction of function of *Tfap2a* and *Tfap2b* affects anxiety, depression, as well as learning and memory (Figures 7 and 8). To assess anxiety-associated behavior, we performed the EPM test (Walf and Frye 2007). Explorative behavior assayed

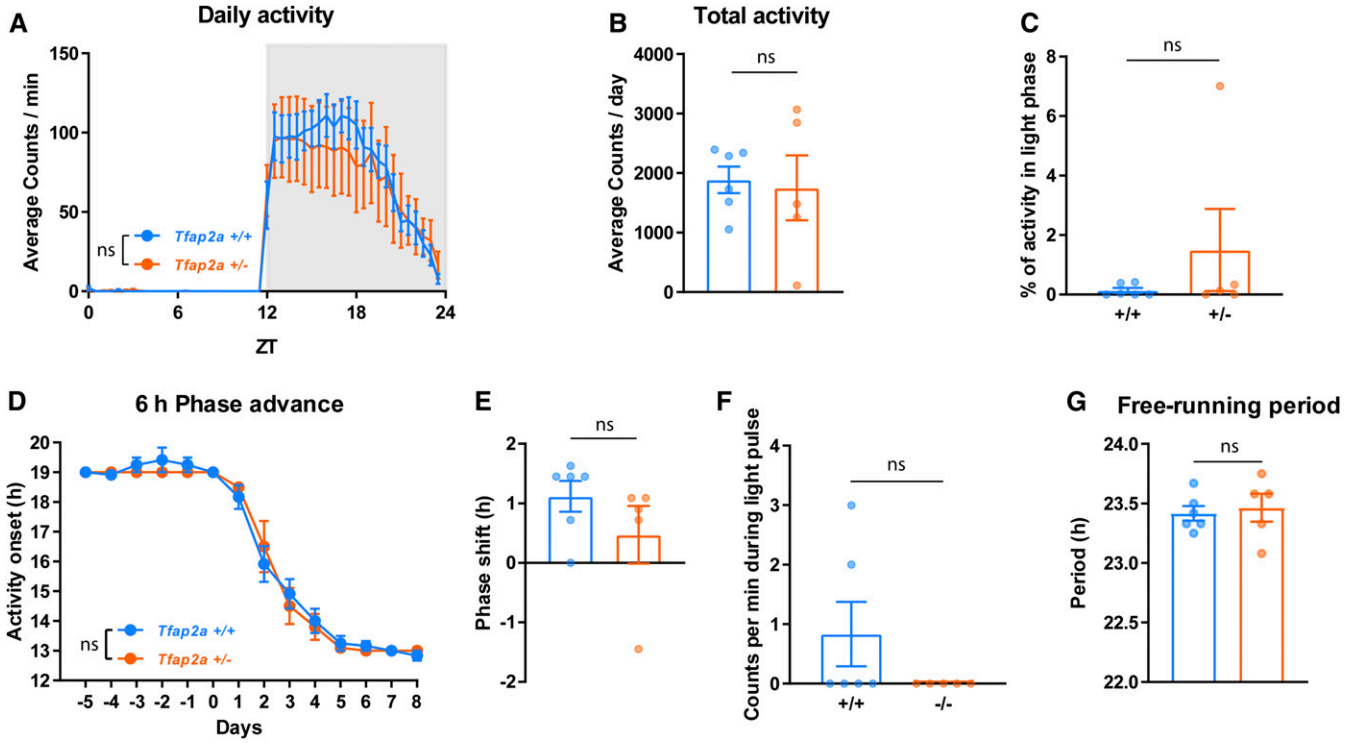

Figure 9 Circadian rhythms are comparable to wild-type controls in *Tfap2a*$^{+/-}$ mice. (A) Daily activity, two-way ANOVA tests followed by Sidak's pairwise comparison, the main effect of genotype: F(1, 432) = 1.133, P = 0.288; the main effect of time, F(47, 432) = 21.64, $P <$ 0.0001. (B) Total activity, P = 0.931, Mann-Whitney test. (C) Activity in light phase, P = 0.784, Mann-Whitney test. (D) Six hours phase advance, Two-way ANOVA tests followed by Sidak's pairwise comparison, the main effect of genotype: F(1, 126) = 0.169, P = 0.682; the main effect of time, F(13, 126) = 156.8, $P <$ 0.0001. (E) Phase shift, P = 0.197, Mann-Whitney test. (F) Locomotor activity during light pulse, P = 0.455, Mann-Whitney test. (G) Free-running period during constant darkness, P = 0.626, Mann-Whitney test. All data are shown as the mean ± SEM n = 6 for *Tfap2a*$^{+/+}$, n = 5 for *Tfap2a*$^{+/-}$.

in the EPM was similar across groups (Figure S8, A–D). The time spent in open arms and entries into the open arms were not changed relative to the corresponding littermates. Thus, we could not detect altered anxiety-associated exploration behavior in *Tfap2a*$^{+/-}$ *or Tfap2b*$^{+/-}$ (Figures 7A and 8A). Accelerating rotarod tests (Deacon 2013) showed that there was no difference in latency to fall during four testing trials in both mutants compared to their respective littermates (Figures 7B and 8B), indicating that motor coordination and balance in both mutants are not affected. Interestingly, *Tfap2b*$^{+/-}$ showed minor motor learning deficiency during the training trials, but this was not observed in *Tfap2a*$^{+/-}$ (Figure S8, E and F).

To assess spatial learning and memory, we performed the MWM test (Radyushkin *et al.* 2009). *Tfap2a*$^{+/-}$ mice as well as controls required similar times to reach the visible platform during the 2 days of training, and the latency was significantly shortened on the second training day (Figure 7C). *Tfap2b*$^{+/-}$ and control mice did not differ significantly when exposed to the visual water maze paradigm (Figure 8C). The mice were next subjected to an 8-day hidden platform training test. Over time, the latency to locate the hidden platform decreased, and the learning pattern in *Tfap2a*$^{+/-}$ mice was comparable to wild-type litter mates (Figure 7D). By contrast, *Tfap2b*$^{+/-}$ mice had severe problems finding the hidden platform (Figure 8D). Finally, the platform was removed in the probe test, and the percentage of time spent in the target quadrant where the platform was previously located was examined in comparison to other quadrants. *Tfap2a*$^{+/-}$ mice and their littermates spent most of the time in the target quadrant, suggesting that they learnt and remembered the previous location of the platform (Figure 7E). By contrast, *Tfap2b*$^{+/-}$ mice did not show the preference for the target quadrant as clearly as the wild type (Figure 8E). Together, these data suggest that spatial learning and memory might be impaired in *Tfap2b*$^{+/-}$ but not in *Tfap2a*$^{+/-}$ mice.Depression-associated behavior was assessed by SPT (Alkhlaif *et al.* 2017), FST (Yankelevitch-Yahav *et al.* 2015) and TST (Can *et al.* 2012). In *Tfap2a*$^{+/-}$ and *Tfap2b*$^{+/-}$ mice, no difference was observed in sucrose preference across all days of the experiment (Figures 7F and 8F). This result suggests that both *Tfap2a*$^{+/-}$ and *Tfap2b*$^{+/-}$ mice are able to experience pleasure from the reward (sucrose water). In the FST, there was no significant difference in latency to immobility and time spent immobile in *Tfap2a*$^{+/-}$ mice, but *Tfap2b*$^{+/-}$ mice showed a reduced immobility latency and spent more time immobile (Figures 7, G–H and 8, G–H). During the TST, increased immobilization latency and less immobility time were observed in *Tfap2a*$^{+/-}$ mutants but not in *Tfap2b*$^{+/-}$ mice (Figures 7, I and J and 8, I and J). Taken together, *Tfap2a*$^{+/-}$ mice showed signs of hyperactive

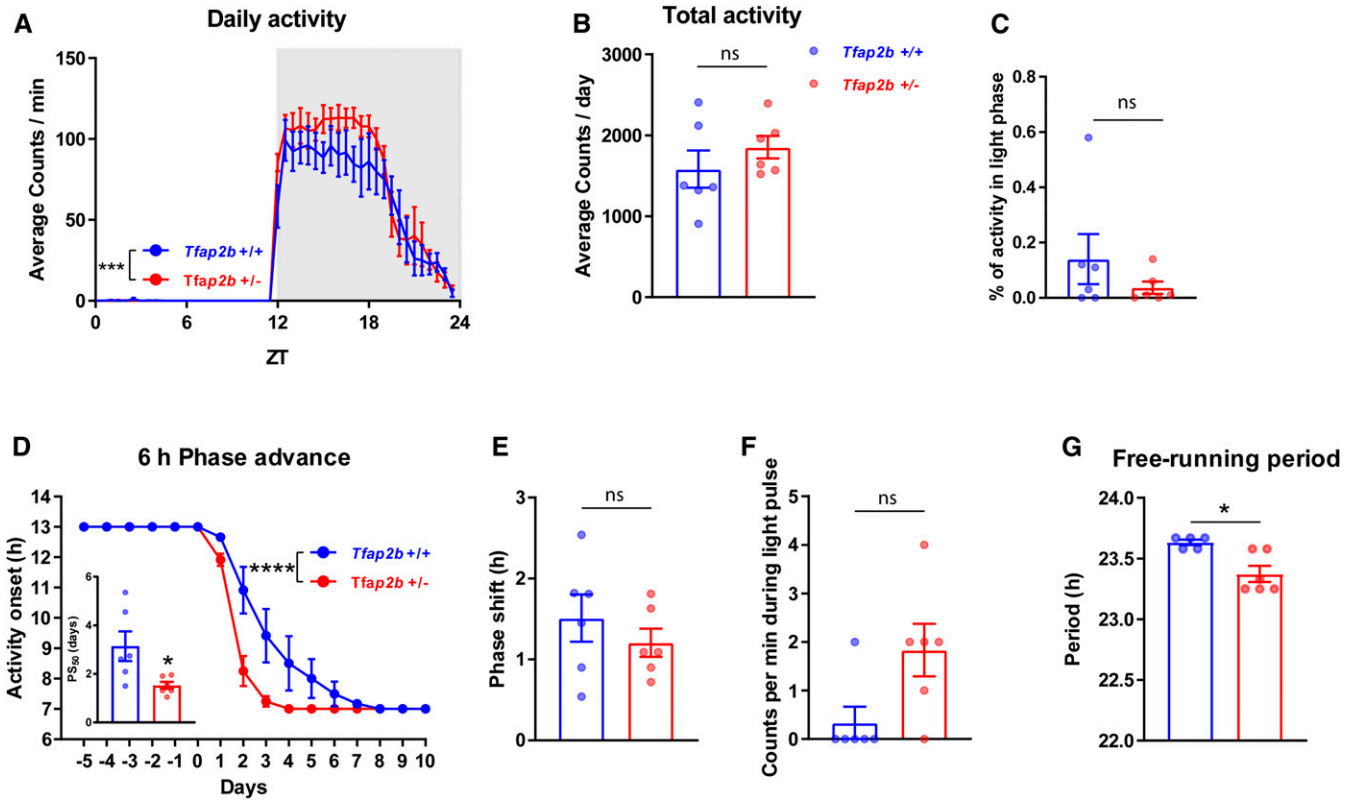

Figure 10 Circadian period is shortened and jetlag re-entrainment is accelerated in *Tfap2b*$^{+/-}$ mice. (A) Daily activity, two-way ANOVA test followed by Sidak's pairwise comparison, the main effect of genotype: F(1, 480) = 13.12, ***P = 0.0003; the main effect of time, F(47, 480) = 65.66, $P <$ 0.0001. (B) Total activity, P = 0.310, Mann-Whitney test. (C) Activity in light phase, P = 0.558, Mann-Whitney test. (D) Six hours phase advance two-way ANOVA test followed by Sidak's pairwise comparison, the main effect of genotype, F(1, 160) = 24.82, ****$P <$ 0.0001; the main effect of time, F(15, 160) = 161.1, $P <$ 0.0001; 50% phase shift (PS_{50}): two-tailed unpaired t-test, *P = 0.0273. (E) Phase shift, P = 0.452, Mann-Whitney test. (F) Locomotor activity during light pulse, P = 0.558, Mann-Whitney test. (G) Free-running period during constant darkness, *P = 0.022, Mann-Whitney test. All data are shown as the mean ± SEM n = 6 for *Tfap2b*$^{+/+}$, n = 6 for *Tfap2b*$^{+/-}$.

behavior in the TST. By contrast, *Tfap2b*$^{+/-}$ mice showed longer periods of immobility in the FST.

We next performed the contextual FC test (Fischer *et al.* 2004). In the conditioning session, average motion and freezing did not differ significantly between mutants and controls in both *Tfap2a*$^{+/-}$ and *Tfap2b*$^{+/-}$ mice. On the first test day after conditioning, both groups of mice showed signs of fear memory as evidenced by increased freezing time. On the second test day, both *Tfap2a*$^{+/-}$ and *Tfap2b*$^{+/-}$ mice exhibited higher motions and less freezing time compared to the respective controls, indicating impaired reconsolidation (Figures 7, K and L and 8, K and L).

In summary, motor function and balance in both *Tfap2a*$^{+/-}$ and *Tfap2b*$^{+/-}$ mice are comparable to wild-type controls. Emotion-associated behavior, assayed by the response to positive sensation (sucrose water) or mild environmental stress (*e.g.*, EPM), in both *Tfap2a*$^{+/-}$ and *Tfap2b*$^{+/-}$ mice also appears to be comparable to wild-type controls. In MWM tests, *Tfap2b*$^{+/-}$ mice showed severe impairment in finding the platform during training. However, the difference between *Tfap2b*$^{+/-}$ and controls was less severe in the probe test, where *Tfap2b*$^{+/-}$ still showed preference of the target quadrant, even though this preference did not reach statistical significance to the neighboring left quadrant. This suggests that, perhaps, spatial memory in *Tfap2b*$^{+/-}$ is less accurate. In addition, the lack of platform arrival might have stimulated expanded search behavior also in other quadrants. Interestingly, *Tfap2a*$^{+/-}$ mice appear to be less stressed when exposed to the TST, whereas *Tfap2b*$^{+/-}$ mice tend to react negatively in this test. *Tfap2b*$^{+/-}$ mice have impaired spatial as well as contextual fear memory. *Tfap2a*$^{+/-}$ mutants have reduced freezing time during FC, but this might be due to the hyperactivity rather than impaired fear memory. These results suggest that the different AP-2 mutants display at least partially divergent behavioral characteristics.

The free-running period of the circadian rhythm is shortened in Tfap2b$^{+/-}$ *mice*

Sleep is strongly regulated by the circadian system. We thus explored circadian rest-activity regulation in *Tfap2a*$^{+/-}$ and *Tfap2b*$^{+/-}$ mice. We measured wheel-running activity under baseline conditions (12 hr light: 12 hr dark - LD), during re-entrainment to a 6 hr phase advance of the LD cycle, in response to a nocturnal light pulse, and under constant dark (DD) conditions (Zheng *et al.* 2001) (Figures 9 and 10). Under LD conditions, *Tfap2a*$^{+/-}$ and *Tfap2b*$^{+/-}$ mice did not show

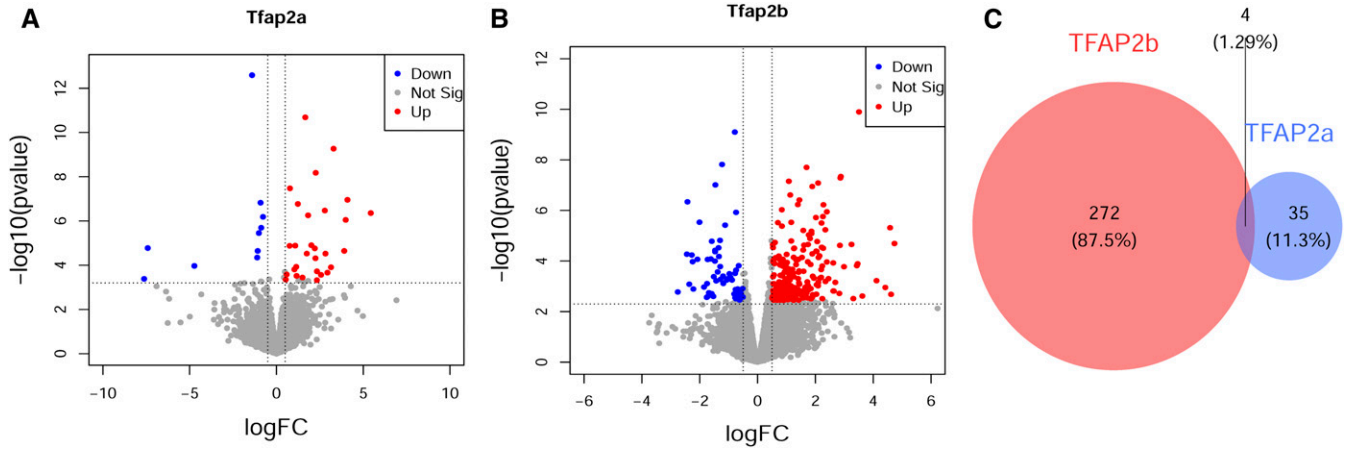

Figure 11 Divergent gene expression changes in *Tfap2a*$^{+/-}$ and *Tfap2b*$^{+/-}$. (A) Volcano plot of genes that are differentially expressed in *Tfap2a*$^{+/-}$ mice. (B) Volcano plot of genes that are differentially expressed in *Tfap2b*$^{+/-}$ mice. (C) Venn diagram showing distinct and overlapping genes that are differentially expressed [false discovery rate (FDR) $<$ 0.20] in *Tfap2a*$^{+/-}$ and *Tfap2b*$^{+/-}$. The overlapping *P* value was calculated using Fischer's Exact tests, $P = 0.005$. $n = 3$ for B6N, $n = 3$ for *Tfap2a*$^{+/-}$, $n = 3$ for *Tfap2b*$^{+/-}$. Genes that are differentially expressed at FDR $<$ 0.20 and logFC $>$ 0.5 are highlighted and labeled in the volcano plot.

significant differences in their rest-activity patterns compared to controls (Figures 9, A–C and 10, A–C). We next measured the response of *Tfap2a*$^{+/-}$ and *Tfap2b*$^{+/-}$ mice to a shift in the LD cycle by advancing the dark phase by 6 hr (jetlag paradigm). Re-entrainment to the new cycle was normal in *Tfap2a*$^{+/-}$ mice compared with wild-type controls (Figure 9D), but it was significantly faster in *Tfap2b*$^{+/-}$ mice (Figure 10D).

To measure the capacity of light to phase reset the circadian clock system of *Tfap2a*$^{+/-}$ and *Tfap2b*$^{+/-}$ mice, a 30-min light pulse was delivered at ZT14 (2 hr after "lights off") and mice were released into DD, which, in wild-type mice, normally induces a phase delay in their rest-activity rhythm (Schwartz and Zimmerman 1990). Light induced similar amounts of phase delays in both *Tfap2a*$^{+/-}$ and *Tfap2b*$^{+/-}$ mice, and the acute reduction of activity during the 30-min light pulse (a.k.a. negative light masking) was not significantly different between mutants and controls (Figures 9, E and F and 10, E and F). There was no difference in DD free-running periods in *Tfap2a*$^{+/-}$ mice, but a shorter period length was observed in *Tfap2b*$^{+/-}$ mice (Figures 9G and 10G). In summary, circadian rhythms in *Tfap2a*$^{+/-}$ mice were comparable to wild-type controls. In *Tfap2b*$^{+/-}$ mice, a shorter intrinsic clock period may have facilitated the faster entrainment in the jetlag paradigm. Speculatively, the observed reduction in sleep amount in these mice might also facilitate such clock acceleration.

Divergent differential gene expression in Tfap2a$^{+/-}$ *and Tfap2b*$^{+/-}$ *mice*

The divergent effects of *Tfap2a*$^{+/-}$ and *Tfap2b*$^{+/-}$ on behavior might stem from different gene expression caused by reduction of the amount of the respective transcription factor. We thus measured gene expression changes in the brain in *Tfap2a*$^{+/-}$, *Tfap2b*$^{+/-}$, and wild type controls. For this, we took brain samples from these mutants and controls, determined their transcriptomes using RNA sequencing, and extracted differentially expressed genes. We found 276 genes to be significantly differentially expressed in *Tfap2b*$^{+/-}$ compared with wild types, whereas only 39 genes were found to be differentially expressed in *Tfap2a*$^{+/-}$. Thus, the more severe behavioral and sleep phenotypes in *Tfap2b*$^{+/-}$ correlate with increased differences in gene expression (Figure 11). Only one gene was downregulated and three genes were upregulated in both *Tfap2a*$^{+/-}$ and *Tfap2b*$^{+/-}$ (Supplemental excel workbook), while all other genes were unique to either of the mutants. This broad divergence in gene expression is consistent with the divergence in sleep and behavior. The differentially expressed genes could potentially explain the sleep and behavioral phenotypes observed in *Tfap2a*$^{+/-}$ and *Tfap2b*$^{+/-}$. We hence searched the literature for these genes to find phenotypes associated with sleep and the behavioral tests that we have performed. Only one gene that is differentially expressed in *Tfap2a*$^{+/-}$ has been previously associated with sleep and none of the genes has been described to have phenotypes in the behavioral tests. By contrast, four genes that are differentially expressed in *Tfap2b*$^{+/-}$ have been associated with sleep phenotypes, and eight genes have been associated with phenotypes in the behavioral tests that we have performed (see details in Table 1). Future studies will be required to establish causality and to solve mechanisms by which *Tfap2a*$^{+/-}$ and *Tfap2b*$^{+/-}$ affect behavior.

Discussion

Divergent phenotypes in sleep, behavior, circadian rhythms, and gene expression in Tfap2a$^{+/-}$ *and Tfap2b*$^{+/-}$

After gene duplication events, paralogs can take on different functions. In mice, both *Tfap2a* and *b* genes play an important role during the development of the neural crest (Mander *et al.* 2013) that gives rise to most of the peripheral nervous system (PNS) and to several non-neural cell types, including

Table 1 Association of *Tfap2b and Tfap2a*-controlled genes with sleep and behavioral phenotypes

		Tfap2a$^{+/-}$	*Tfap2b*$^{+/-}$	
Assay	Phenotype	DE genes	Phenotype	DE genes
EEG/EMG recording	Normal sleep amount but increased sleep power	Slc5a5[a]	Shortened sleep amount and impaired sleep quality	Fos[a], Fosb[a], Slc5a5[a] Slc18a2[b]
EPM	Normal anxiety-associated behavior	—	Normal anxiety-associated behavior	—
Rotarod	Normal motor function	—	Normal motor function	—
MWM	Normal spatial learning and memory	—	Impaired spatial learning and memory	Arc[a], Fos[a], Fosb[a], Vgf[a]
SPT, FST, TST	Hyperactive in TST, but normal in SPT or TST	—	Depression-like behavior only in FST, but normal in SPT or TST	Fosb[a], Dusp1[a] Slc6a4[b]
Contextual fear conditioning	Shortened freezing behavior	—	Shortened freezing behavior	Arc[a], Vgf[a] Slc6a4[b]
Wheel-running	Normal circadian activity	—	Shortened circadian period and accelerated re-entrainment	Vgf[a]

Literature analysis of genes that are differentially expressed in *Tfap2a*$^{+/-}$ and *TFAP2b*$^{+/-}$. All interpretations are purely speculative. *Fos* and *Fosb* from the *Fos* family of transcription factors as well as *Slc5a5* and *Slc18a2* from the solute carrier (SLC) group of membrane transport proteins were found to be differentially regulated in *Tfap2b*$^{+/-}$ mice, which might contribute to the shortened sleep (Figure 3). *Slc5a5*, which encodes a sodium/iodide symporter (NIS), was down regulated in both *Tfap2a*$^{+/-}$ and *Tfap2b*$^{+/-}$ mice. The NIS plays a fundamental role in the first step in thyroid hormone biosynthesis (Dohán *et al.* 2003). Multiple phenotypes relating to neurological features, skeleton, vision, and metabolism have been discovered in *Slc5a5* knockouts. Among those phenotypes, abnormal sleep behavior, such as shorter sleep bout duration during the dark phase, has been found in male *Slc5a5*$^{-/-}$ mice (Dickinson *et al.* 2016). *Fos* (*c-fos*) is a nuclear proto-oncogene, whose expression is used as an indirect marker of neuronal activity. *Fosb* expression is induced often in the same cells as *Fos*, but at a later time (Gass *et al.* 1992; Peters *et al.* 1994). In *Tfap2b*$^{+/-}$ mice, *Fos* and *Fosb* were downregulated. Abnormal sleep has been found in *Fos* or Fosb-deficient mice such that *Fos-null* mice have less NREMS and normal REM sleep, but *Fosb*-deficient mice have less REMS but unchanged NREMS (Shiromani *et al.* 2000). Dopamine is transported into synaptic vesicles by the vesicular monoamine transporter (VMAT2), which is encoded by *Slc18a2*. VMAT2-deficient mice are used as a model of Parkinson's Disease (PD) that exhibits shorter latency to sleep and lower circadian activity except for a major phenotype of the motor dysfunction (Taylor *et al.* 2009). In *Tfap2b*$^{+/-}$ animals, *Slc18a2* was upregulated, and overexpression of this gene was reported to have neuroprotective effects, such as antidepressive and anxiolytic activity and increased ambulation during the dark phase (Lohr *et al.* 2014). The downregulation of *Arc*, *Fos*, *Fosb*, and *Vgf* might be associated with the impaired spatial learning and memory that we found in *Tfap2b*$^{+/-}$ animals (Figure 8, C–E). The deletion of either *Arc*, *Fos*, *Fosb*, or *Vgf* in mice result in impaired spatial learning (Paylor *et al.* 1994; Plath *et al.* 2006; Bozdagi *et al.* 2008; Ohnishi *et al.* 2011). Increased immobility was observed in *Tfap2b*$^{+/-}$ mice (Figure 8H), which is consistent with downregulation of *Fosb* and *Dusp1* as well as upregulation of *Slc6a4*. *Fosb* null mice have increased immobility in FST compared with their controls (Ohnishi *et al.* 2011). On the contrary, overexpression of *Dusp1* causes depressive behaviors and mice lacking *Dusp-1* are resilient to stress (Duric *et al.* 2010). *Slc6a4* encodes the serotonin transporter (SERT) in mice. It is reported that mice that are more susceptible to stress have increased expression of SERT and exhibit longer immobility in FST (Couch *et al.* 2013). In addition, SERT overexpression (5-HTTOE) mice have reduced freezing time in the cued fear conditioning test (McHugh *et al.* 2015). In *Tfap2b*$^{+/-}$ mice, we found a shortened freezing time in the contextual fear conditioning test (Figure 8L). The downregulation of *Arc* and *Vgf* might also contribute to this fear-related phenotype, as *Arc* and *Vgf* null mice exhibit shortened freezing time in the contextual fear conditioning test (Plath *et al.* 2006; Bozdagi *et al.* 2008). Moreover, *Vgf*$^{-/-}$ mice have a slightly shortened circadian period length (Hahm *et al.* 1999), which might help explain the similar phenotype we observed in *Tfap2b*$^{+/-}$ mice (Figure 10).

[a] Upregulated genes.

[b] Downregulated genes. "—" indicates that no information was found.

smooth muscle cells of the cardiovascular system, pigment cells in the skin, and craniofacial bones (Moser *et al.* 1997b). Despite their common expression pattern during early embryonic stages, deletion of *Tfap2a* or *Tfap2b* produces strikingly different phenotypes (Zhang *et al.* 1996). The loss of *Tfap2a* causes neuronal, craniofacial, skeletal, and body wall defects, whereas *Tfap2b*-deficient mice show brain development, *ductus arteriosus*, and renal impairments (Zhang *et al.* 1996; Moser *et al.* 1997a; Brewer *et al.* 2004).

Functional divergence in AP-2 is also seen for sleep phenotypes. *Tfap2a*$^{+/-}$ displays a rather increased sleep quality, whereas sleep length and quality in *Tfap2b*$^{+/-}$ are reduced. Homeostatic regulation exists in both *Tfap2a*$^{+/-}$ *and Tfap2b*$^{+/-}$, but a stronger response was found in the former and a weaker one in the latter. Our work from *C. elegans* and *Drosophila* indicated that the ancient function of AP-2 appears to be to promote sleep (Turek *et al.* 2013; Kucherenko *et al.* 2016). This suggests that *Tfap2b*$^{+/-}$ may have kept the original sleep-promoting function, whereas *Tfap2a*$^{+/-}$ may have taken on a new, opposing function in sleep control. Thus, as sleep evolved in more complex brains, there might have emerged a need for negative control of sleep that favored the divergence of AP-2 transcription factors.

We show that this functional divergence extended to additional behaviors. *Tfap2a*$^{+/-}$ was more robust in the behavioral assays, at least in the TST, which indicated a mild hyperactivity. By contrast, the performance of *Tfap2b*$^{+/-}$ revealed mildly depressive-like symptoms. Consistent with diverging roles in development and behavior, our RNA-sequencing data of *Tfap2a*$^{+/-}$ and *Tfap2b*$^{+/-}$ mice revealed divergent patterns of gene expression. The divergent behavioral changes observed in *Tfap2a*$^{+/-}$ *and Tfap2b*$^{+/-}$ mice may, thus, speculatively result from the modulation of expression of *Tfap2a* and *Tfap2b* target genes. Consistent with this view, *Tfap2a* and *Tfap2b* have been shown to play distinct roles in the specification of GABAergic neurons (Zainolabidin *et al.* 2017). This finding is intriguing as sleep-active, sleep-inducing neurons typically are GABAergic. Alternatively, changes in depressive-like symptoms in the mutants may be the consequence of sleep quality alterations. As poor sleep quality impairs memory consolidation (Mander *et al.* 2013; Bezdicek *et al.* 2018), the memory deficits shown in *Tfap2b*$^{+/-}$ mice might be the result

of a loss of sleep time or quality. *Tfap2a*$^{+/-}$ mice showed less freezing in FC despite a better sleep quality. However, since *Tfap2a*$^{+/-}$ mice exhibited hyperactive behavior in a stressful situation (TST), this effect might speculatively have blunted the freezing response in FC.

Different phenotypes were also found in circadian rhythm regulation for *Tfap2a*$^{+/-}$ *and Tfap2b*$^{+/-}$ mice. Circadian rhythmicity was unaffected in *Tfap2a*$^{+/-}$, whereas *Tfap2b*$^{+/-}$ showed a shortened period of the internal clock system. The circadian period shortening in *Tfap2b*$^{+/-}$ most likely is too mild to be the cause of the sleep impairment. For example, mice lacking the clock gene *Per1* with 1 hr shorter intrinsic period and preserved homeostatic responses do not exhibit overall sleep changes (Kopp *et al.* 2002).

Our results suggest that AP-2 transcription factors have diverged to take on divergent control of sleep and other behaviors. To our knowledge, this is the first instance where a sleep gene is shown to have diversified in evolution from a sleep-promoting role in invertebrates to serve bidirectional control of sleep in mammals.

Acknowledgments

We thank Ahmed Mansouri, Mayumi Kimura, Anja Ronnenberg, Ulrike Teichmann, and Sara Kimmina for advice on electroencephalogram (EEG), animal experimentation, and help with obtaining permits. We are grateful to Gregor Eichele for providing laboratory space and resources. We thank Markus Moser and Trever Williams for mouse strains. Sequencing was carried out by Bernd Timmermann and Stefan Börno, Max Planck Institute for Molecular Genetics, Berlin. This work was supported by the Max Planck Society (Max Planck Research Group "Sleep and Waking"), by a European Research Council Starting Grant (ID: 637860, SLEEPCONTROL), and by Deutsche Forschungsgemeinschaft (DFG) grants AS547/1-1 and OS353-10/1.

Literature Cited

Alkhlaif, Y., D. Bagdas, A. Jackson, A. J. Park, and I. M. Damaj, 2017 Assessment of nicotine withdrawal-induced changes in sucrose preference in mice. Pharmacol. Biochem. Behav. 161: 47–52. https://doi.org/10.1016/j.pbb.2017.08.013

Bernard, K., N. J. Logsdon, S. Ravi, N. Xie, B. P. Persons *et al.*, 2015 Metabolic reprogramming is required for myofibroblast contractility and differentiation. J. Biol. Chem. 290: 25427–25438. https://doi.org/10.1074/jbc.M115.646984

Bezdicek, O., T. Nikolai, J. Nepozitek, P. Perinova, D. Kemlink *et al.*, 2018 Prospective memory impairment in idiopathic REM sleep behavior disorder. Clin. Neuropsychol. 32: 1019–1037. https://doi.org/10.1080/13854046.2017.1394493

Bozdagi, O., E. Rich, S. Tronel, M. Sadahiro, K. Patterson *et al.*, 2008 The neurotrophin-inducible gene Vgf regulates hippocampal function and behavior through a brain-derived neurotrophic factor-dependent mechanism. J. Neurosci. 28: 9857–9869. https://doi.org/10.1523/JNEUROSCI.3145-08.2008

Brewer, S., W. Feng, J. Huang, S. Sullivan, and T. Williams, 2004 Wnt1-Cre-mediated deletion of AP-2alpha causes multiple neural crest-related defects. Dev. Biol. 267: 135–152. https://doi.org/10.1016/j.ydbio.2003.10.039

Bringmann, H., 2018 Sleep-active neurons: conserved motors of sleep. Genetics 208: 1279–1289. https://doi.org/10.1534/genetics.117.300521

Campbell, S. S., and I. Tobler, 1984 Animal sleep: a review of sleep duration across phylogeny. Neurosci. Biobehav. Rev. 8: 269–300. https://doi.org/10.1016/0149-7634(84)90054-X

Can, A., D. T. Dao, C. E. Terrillion, S. C. Piantadosi, S. Bhat *et al.*, 2012 The tail suspension test. J. Vis. Exp. 59: e 3769. https://doi.org/10.3791/3769

Chazaud, C., M. Oulad-Abdelghani, P. Bouillet, D. Decimo, P. Chambon *et al.*, 1996 AP-2.2, a novel gene related to AP-2, is expressed in the forebrain, limbs and face during mouse embryogenesis. Mech. Dev. 54: 83–94. https://doi.org/10.1016/0925-4773(95)00463-7

Colavito, V., P. F. Fabene, G. Grassi-Zucconi, F. Pifferi, Y. Lamberty *et al.*, 2013 Experimental sleep deprivation as a tool to test memory deficits in rodents. Front. Syst. Neurosci. 7: 106. https://doi.org/10.3389/fnsys.2013.00106

Couch, Y., D. C. Anthony, O. Dolgov, A. Revischin, B. Festoff *et al.*, 2013 Microglial activation, increased TNF and SERT expression in the prefrontal cortex define stress-altered behaviour in mice susceptible to anhedonia. Brain Behav. Immun. 29: 136–146 [Corrigenda: Brain Behav. Immun. 36: 215 (2014)]. https://doi.org/10.1016/j.bbi.2012.12.017

Deacon, R. M., 2013 Measuring motor coordination in mice. J. Vis. Exp. 75: e 2609. https://doi.org/10.3791/2609

Dickinson, M. E., A. M. Flenniken, X. Ji, L. Teboul, M. D. Wong *et al.*, 2016 High-throughput discovery of novel developmental phenotypes. Nature 537: 508–514 [Corrigenda: Nature 551: 398 (2017)]. https://doi.org/10.1038/nature19356

Dobin, A., C. A. Davis, F. Schlesinger, J. Drenkow, C. Zaleski *et al.*, 2013 STAR: ultrafast universal RNA-seq aligner. Bioinformatics 29: 15–21. https://doi.org/10.1093/bioinformatics/bts635

Dohán, O., A. De la Vieja, V. Paroder, C. Riedel, M. Artani *et al.*, 2003 The sodium/iodide Symporter (NIS): characterization, regulation, and medical significance. Endocr. Rev. 24: 48–77. https://doi.org/10.1210/er.2001-0029

Duric, V., M. Banasr, P. Licznerski, H. D. Schmidt, C. A. Stockmeier *et al.*, 2010 A negative regulator of MAP kinase causes depressive behavior. Nat. Med. 16: 1328–1332. https://doi.org/10.1038/nm.2219

Eckert, D., S. Buhl, S. Weber, R. Jager, and H. Schorle, 2005 The AP-2 family of transcription factors. Genome Biol. 6: 246. https://doi.org/10.1186/gb-2005-6-13-246

Fischer, A., F. Sananbenesi, C. Schrick, J. Spiess, and J. Radulovic, 2004 Distinct roles of hippocampal de novo protein synthesis and actin rearrangement in extinction of contextual fear. J. Neurosci. 24: 1962–1966. https://doi.org/10.1523/JNEUROSCI.5112-03.2004

Funato, H., C. Miyoshi, T. Fujiyama, T. Kanda, M. Sato *et al.*, 2016 Forward-genetics analysis of sleep in randomly mutagenized mice. Nature 539: 378–383. https://doi.org/10.1038/nature20142

Gao, V., F. Turek, and M. Vitaterna, 2016 Multiple classifier systems for automatic sleep scoring in mice. J. Neurosci. Methods 264: 33–39. https://doi.org/10.1016/j.jneumeth.2016.02.016

Gass, P., T. Herdegen, R. Bravo, and M. Kiessling, 1992 Induction of immediate early gene encoded proteins in the rat hippocampus after bicuculline-induced seizures: differential expression of KROX-24, FOS and JUN proteins. Neuroscience 48: 315–324. https://doi.org/10.1016/0306-4522(92)90493-L

Gibney, P. A., C. Lu, A. A. Caudy, D. C. Hess, and D. Botstein, 2013 Yeast metabolic and signaling genes are required for heat-shock survival and have little overlap with the heat-in-

duced genes. Proc. Natl. Acad. Sci. USA 110: E4393–E4402. https://doi.org/10.1073/pnas.1318100110

Green, R. M., W. Feng, T. Phang, J. L. Fish, H. Li *et al.*, 2015 Tfap2a-dependent changes in mouse facial morphology result in clefting that can be ameliorated by a reduction in Fgf8 gene dosage. Dis. Model. Mech. 8: 31–43. https://doi.org/10.1242/dmm.017616

Grubbs, J. J., L. L. Lopes, A. M. van der Linden, and D. M. Raizen, 2019 Sik-Hdac4 signaling is required for the metabolic regulation of sleep. Sleep 42: A11.

Hahm, S., T. M. Mizuno, T. J. Wu, J. P. Wisor, C. A. Priest *et al.*, 1999 Targeted deletion of the Vgf gene indicates that the encoded secretory peptide precursor plays a novel role in the regulation of energy balance. Neuron 23: 537–548. https://doi.org/10.1016/S0896-6273(00)80806-5

Joiner, W. J., 2016 Unraveling the evolutionary determinants of sleep. Curr. Biol. 26: R1073–R1087. https://doi.org/10.1016/j.cub.2016.08.068

Keene, A. C., and E. R. Duboue, 2018 The origins and evolution of sleep. J. Exp. Biol. 221: jeb159533. https://doi.org/10.1242/jeb.159533

Kent, B. A., S. M. Strittmatter, and H. B. Nygaard, 2018 Sleep and EEG power spectral analysis in three transgenic mouse models of Alzheimer's disease: APP/PS1, 3xTgAD, and Tg2576. J. Alzheimers Dis. 64: 1325–1336. https://doi.org/10.3233/JAD-180260

Kohlbecker, A., A. E. Lee, and H. Schorle, 2002 Exencephaly in a subset of animals heterozygous for AP-2alpha mutation. Teratology 65: 213–218. https://doi.org/10.1002/tera.10037

Kopp, C., U. Albrecht, B. Zheng, and I. Tobler, 2002 Homeostatic sleep regulation is preserved in mPer1 and mPer2 mutant mice. Eur. J. Neurosci. 16: 1099–1106. https://doi.org/10.1046/j.1460-9568.2002.02156.x

Kucherenko, M. M., V. Ilangovan, B. Herzig, H. R. Shcherbata, and H. Bringmann, 2016 TfAP-2 is required for night sleep in Drosophila. BMC Neurosci. 17: 72. https://doi.org/10.1186/s12868-016-0306-3

Lin, J. M., E. Z. M. Taroc, J. A. Frias, A. Prasad, A. N. Catizone *et al.*, 2018 The transcription factor Tfap2e/AP-2ε plays a pivotal role in maintaining the identity of basal vomeronasal sensory neurons. Dev. Biol. 441: 67–82. https://doi.org/10.1016/j.ydbio.2018.06.007

Li, H., R. Sheridan, and T. Williams, 2013 Analysis of TFAP2A mutations in Branchio-Oculo-Facial Syndrome indicates functional complexity within the AP-2alpha DNA-binding domain. Hum. Mol. Genet. 22: 3195–3206. https://doi.org/10.1093/hmg/ddt173

Lohr, K. M., A. I. Bernstein, K. A. Stout, A. R. Dunn, C. R. Lazo *et al.*, 2014 Increased vesicular monoamine transporter enhances dopamine release and opposes Parkinson disease-related neurodegeneration in vivo. Proc. Natl. Acad. Sci. USA 111: 9977–9982. https://doi.org/10.1073/pnas.1402134111

Mander, B. A., V. Rao, B. Lu, J. M. Saletin, J. R. Lindquist *et al.*, 2013 Prefrontal atrophy, disrupted NREM slow waves and impaired hippocampal-dependent memory in aging. Nat. Neurosci. 16: 357–364. https://doi.org/10.1038/nn.3324

Mang, G. M., and P. Franken, 2012 Sleep and EEG phenotyping in mice. Curr. Protoc. Mouse Biol. 2: 55–74.

Mani, A., J. Radhakrishnan, A. Farhi, K. S. Carew, C. A. Warnes *et al.*, 2005 Syndromic patent ductus arteriosus: evidence for haploinsufficient TFAP2B mutations and identification of a linked sleep disorder. Proc. Natl. Acad. Sci. USA 102: 2975–2979. https://doi.org/10.1073/pnas.0409852102

Martin, M., 2011 Cutadapt removes adapter sequences from high-throughput sequencing reads. 17: 3.

Matsuda, R., T. Kohno, S. Kohsaka, R. Fukuoka, Y. Maekawa *et al.*, 2017 The prevalence of poor sleep quality and its association with depression and anxiety scores in patients admitted for cardiovascular disease: a cross-sectional designed study. Int. J. Cardiol. 228: 977–982. https://doi.org/10.1016/j.ijcard.2016.11.091

McHugh, S. B., C. Barkus, J. Lima, L. R. Glover, T. Sharp *et al.*, 2015 SERT and uncertainty: serotonin transporter expression influences information processing biases for ambiguous aversive cues in mice. Genes Brain Behav. 14: 330–336. https://doi.org/10.1111/gbb.12215

Miyazaki, S., C. Y. Liu, and Y. Hayashi, 2017 Sleep in vertebrate and invertebrate animals, and insights into the function and evolution of sleep. Neurosci. Res. 118: 3–12. https://doi.org/10.1016/j.neures.2017.04.017

Moser, M., A. Pscherer, C. Roth, J. Becker, G. Mucher *et al.*, 1997a Enhanced apoptotic cell death of renal epithelial cells in mice lacking transcription factor AP-2beta. Genes Dev. 11: 1938–1948. https://doi.org/10.1101/gad.11.15.1938

Moser, M., J. Ruschoff, and R. Buettner, 1997b Comparative analysis of AP-2 alpha and AP-2 beta gene expression during murine embryogenesis. Dev. Dyn. 208: 115–124. https://doi.org/10.1002/(SICI)1097-0177(199701)208:1<115::AID-AJA11>3.0.CO;2-5

Ohnishi, Y. N., Y. H. Ohnishi, M. Hokama, H. Nomaru, K. Yamazaki *et al.*, 2011 FosB is essential for the enhancement of stress tolerance and antagonizes locomotor sensitization by DeltaFosB. Biol. Psychiatry 70: 487–495. https://doi.org/10.1016/j.biopsych.2011.04.021

Paylor, R., R. S. Johnson, V. Papaioannou, B. M. Spiegelman, and J. M. Wehner, 1994 Behavioral assessment of c-fos mutant mice. Brain Res. 651: 275–282. https://doi.org/10.1016/0006-8993(94)90707-2

Peters, R. V., N. Aronin, and W. J. Schwartz, 1994 Circadian regulation of Fos B is different from c-Fos in the rat suprachiasmatic nucleus. Brain Res. Mol. Brain Res. 27: 243–248. https://doi.org/10.1016/0169-328X(94)90006-X

Plath, N., O. Ohana, B. Dammermann, M. L. Errington, D. Schmitz *et al.*, 2006 Arc/Arg3.1 is essential for the consolidation of synaptic plasticity and memories. Neuron 52: 437–444. https://doi.org/10.1016/j.neuron.2006.08.024

Radyushkin, K., K. Hammerschmidt, S. Boretius, F. Varoqueaux, A. El-Kordi *et al.*, 2009 Neuroligin-3-deficient mice: model of a monogenic heritable form of autism with an olfactory deficit. Genes Brain Behav. 8: 416–425. https://doi.org/10.1111/j.1601-183X.2009.00487.x

Raizen, D. M., and J. E. Zimmerman, 2011 Non-mammalian genetic model systems in sleep research. Sleep Med. Clin. 6: 131–139. https://doi.org/10.1016/j.jsmc.2011.04.005

Roberts, G. G., 3rd, and A. P. Hudson, 2009 Rsf1p is required for an efficient metabolic shift from fermentative to glycerol-based respiratory growth in S. cerevisiae. Yeast 26: 95–110. https://doi.org/10.1002/yea.1655

Sananbenesi, F., A. Fischer, X. Wang, C. Schrick, R. Neve *et al.*, 2007 A hippocampal Cdk5 pathway regulates extinction of contextual fear. Nat. Neurosci. 10: 1012–1019. https://doi.org/10.1038/nn1943

Satoda, M., M. E. Pierpont, G. A. Diaz, R. A. Bornemeier, and B. D. Gelb, 1999 Char syndrome, an inherited disorder with patent ductus arteriosus, maps to chromosome 6p12-p21. Circulation 99: 3036–3042. https://doi.org/10.1161/01.CIR.99.23.3036

Satoda, M., F. Zhao, G. A. Diaz, J. Burn, J. Goodship *et al.*, 2000 Mutations in TFAP2B cause Char syndrome, a familial form of patent ductus arteriosus. Nat. Genet. 25: 42–46. https://doi.org/10.1038/75578

Schorle, H., P. Meier, M. Buchert, R. Jaenisch, and P. J. Mitchell, 1996 Transcription factor AP-2 essential for cranial closure and craniofacial development. Nature 381: 235–238. https://doi.org/10.1038/381235a0

Schwartz, W. J., and P. Zimmerman, 1990 Circadian timekeeping in BALB/c and C57BL/6 inbred mouse strains. J. Neurosci. 10: 3685–3694. https://doi.org/10.1523/JNEUROSCI.10-11-03685.1990

Shiromani, P. J., R. Basheer, J. Thakkar, D. Wagner, M. A. Greco *et al.*, 2000 Sleep and wakefulness in c-fos and fos B gene knockout mice. Brain Res. Mol. Brain Res. 80: 75–87. https://doi.org/10.1016/S0169-328X(00)00123-6

Taylor, T. N., W. M. Caudle, K. R. Shepherd, A. Noorian, C. R. Jackson *et al.*, 2009 Nonmotor symptoms of Parkinson's disease revealed in an animal model with reduced monoamine storage capacity. J. Neurosci. 29: 8103–8113. https://doi.org/10.1523/JNEUROSCI.1495-09.2009

Tobler, I., 1995 Is sleep fundamentally different between mammalian species? Behav. Brain Res. 69: 35–41. https://doi.org/10.1016/0166-4328(95)00025-O

Turek, M., I. Lewandrowski, and H. Bringmann, 2013 An AP2 transcription factor is required for a sleep-active neuron to induce sleep-like quiescence in C. elegans. Curr. Biol. 23: 2215–2223. https://doi.org/10.1016/j.cub.2013.09.028

Verbitsky, E. V., 2017 Anxiety and sleep in experiment and clinic. Zh. Nevrol. Psikhiatr. Im. S. S. Korsakova 117: 12–18. https://doi.org/10.17116/jnevro20171174212-18

Walf, A. A., and C. A. Frye, 2007 The use of the elevated plus maze as an assay of anxiety-related behavior in rodents. Nat. Protoc. 2: 322–328. https://doi.org/10.1038/nprot.2007.44

Werling, U., and H. Schorle, 2002 Transcription factor gene AP-2 gamma essential for early murine development. Mol. Cell. Biol. 22: 3149–3156. https://doi.org/10.1128/MCB.22.9.3149-3156.2002

Williams, T., and R. Tjian, 1991 Characterization of a dimerization motif in AP-2 and its function in heterologous DNA-binding proteins. Science 251: 1067–1071. https://doi.org/10.1126/science.1998122

Yankelevitch-Yahav, R., M. Franko, A. Huly, and R. Doron, 2015 The forced swim test as a model of depressive-like behavior. J. Vis. Exp. 97: 52587. https://doi.org/10.3791/52587

Zainolabidin, N., S. P. Kamath, A. R. Thanawalla, and A. I. Chen, 2017 Distinct activities of Tfap2A and Tfap2B in the specification of GABAergic interneurons in the developing cerebellum. Front. Mol. Neurosci. 10: 281. https://doi.org/10.3389/fnmol.2017.00281

Zhang, J., S. Hagopian-Donaldson, G. Serbedzija, J. Elsemore, D. Plehn-Dujowich *et al.*, 1996 Neural tube, skeletal and body wall defects in mice lacking transcription factor AP-2. Nature 381: 238–241. https://doi.org/10.1038/381238a0

Zhao, F., C. G. Weismann, M. Satoda, M. E. Pierpont, E. Sweeney *et al.*, 2001 Novel TFAP2B mutations that cause Char syndrome provide a genotype-phenotype correlation. Am. J. Hum. Genet. 69: 695–703. https://doi.org/10.1086/323410

Zhao, F., T. Lufkin, and B. D. Gelb, 2003 Expression of Tfap2d, the gene encoding the transcription factor Ap-2 delta, during mouse embryogenesis. Gene Expr. Patterns 3: 213–217. https://doi.org/10.1016/S1567-133X(02)00067-4

Zheng, B., U. Albrecht, K. Kaasik, M. Sage, W. Lu *et al.*, 2001 Nonredundant roles of the mPer1 and mPer2 genes in the mammalian circadian clock. Cell 105: 683–694. https://doi.org/10.1016/S0092-8674(01)00380-4

Communicating editor: J. Schimenti